Received: 13 December 2021 | Revised: 6 June 2022 | Accepted: 11 June 2022

DOI: 10.1111/bre.12691

Basin Research | IAS EAGE | WILEY

RESEARCH ARTICLE

Low-temperature thermal history of the McArthur Basin: Influence of the Cambrian Kalkarindji Large Igneous Province on hydrocarbon maturation

Angus L. Nixon[1,2] | **Stijn Glorie**[1,2] | **Derrick Hasterok**[1] | **Alan S. Collins**[1,2] | **Nicholas Fernie**[3] | **Geoffrey Fraser**[4]

[1]Department of Earth Science, School of Physical Sciences, The University of Adelaide, Adelaide, South Australia, Australia

[2]Mineral Exploration Cooperative Research Centre, Department of Earth Sciences, The University of Adelaide, Adelaide, South Australia, Australia

[3]Santos, Adelaide, South Australia, Australia

[4]Minerals, Energy and Groundwater Division, Geoscience Australia, Canberra, ACT, Australia

Correspondence
Angus L. Nixon, Department of Earth Science, School of Physical Sciences, The University of Adelaide, Adelaide, SA 5005, Australia.
Email: angus.nixon@adelaide.edu.au

Funding information
Australian Research Council, Grant/Award Number: LP160101353 and LE150100145; MinEx CRC (Mineral Exploration Cooperative Research Centre)

Abstract

The McArthur Basin of the North Australian Craton is one of the very few places on Earth where extensive hydrocarbons are preserved that were generated from Mesoproterozoic source rocks, prior to the development of extensive multicellular life. It is, however, unclear precisely when hydrocarbons from these source rocks matured, and if this occurred as a singular event or multiple phases. In this study, we present new apatite fission track data from a combination of outcrop and sub-surface samples from the McArthur Basin to investigate the post-depositional thermal history of the basin, and to explore the timing of hydrocarbon maturation. Apatite fission track data and thermal modelling suggest that the McArthur Basin experienced a basin-wide reheating event contemporaneous with the eruption of the Cambrian Kalkarindji Large Igneous Province in the North and West Australian cratons, during which thick (>500 m) basaltic flows blanketed the basin surface. Reheating at ca. 510 Ma coinciding with Kalkarindji volcanism is consistent with a proposed timing of elevated hydrocarbon maturation, particularly in the Beetaloo Sub-basin, and provides a mechanism for petroleum generation throughout the basin. Subsequent regional cooling was slow and gradual, most likely facilitated by gentle erosion (ca. 0.01–0.006 km/Ma) of overlying Georgina Basin sediments in the Devonian–Carboniferous with little structural reactivation. This model provides a framework in which hydrocarbons, sourced from Mesoproterozoic carbon-rich rocks, may have experienced thermal maturation much later in the Cambrian. Preservation of these hydrocarbons was aided by a lack of widespread structural exhumation following this event.

KEYWORDS

apatite fission track, Beetaloo Sub-basin, exhumation, hydrocarbon maturity, Kalkarindji Large Igneous Province, McArthur Basin, thermal history

This is an open access article under the terms of the Creative Commons Attribution License, which permits use, distribution and reproduction in any medium, provided the original work is properly cited.
© 2022 The Authors. *Basin Research* published by International Association of Sedimentologists and European Association of Geoscientists and Engineers and John Wiley & Sons Ltd.

13652117, 2022, 6, Downloaded from https://onlinelibrary.wiley.com/doi/10.1111/bre.12691 by University of Adelaide Alumni, Wiley Online Library on [28/11/2022]. See the Terms and Conditions (https://onlinelibrary.wiley.com/terms-and-conditions) on Wiley Online Library for rules of use; OA articles are governed by the applicable Creative Commons License

1 | INTRODUCTION

The Palaeoproterozoic–Mesoproterozoic McArthur Basin in northern Australia has been the subject of considerable study into syn-depositional basin processes and conditions, from which a confident understanding of the prolonged sedimentary system is emerging (see Cox et al., 2022, for an overview). Overlying Palaeoproterozoic basement of the North Australian Craton, the McArthur Basin is an unmetamorphosed and largely undeformed sequence of sedimentary and volcanic rocks deposited over a period of more than 500 million years (e.g., Ahmad & Munson, 2013; Rawlings, 1999; Yang, Collins, Blades, et al., 2020). Intriguingly, the basin hosts considerable hydrocarbon reserves derived from Mesoproterozoic source rocks, which have been preserved to the present day (Cox et al., 2016, 2022; Jackson et al., 1986). While extensive research has been undertaken characterising the hydrocarbon source, chemistry and maturity (e.g., Cox et al., 2022; Crick et al., 1988; George et al., 1994; Jackson & Raiswell, 1991; Lanigan et al., 1994; Summons et al., 1988), the timing of hydrocarbon maturation remains poorly resolved. Consequently, the preservation of hydrocarbons produced from Mesoproterozoic source rocks in the McArthur Basin remains a fundamental and unresolved question.

A key parameter in understanding this hydrocarbon preservation is the post-depositional thermal history of the basin. Yet, only very limited direct assessment of basin thermal evolution has been undertaken (Duddy et al., 2004), which does not resolve the basin thermal history prior to the Mesozoic. Consequently, estimates for the timing of hydrocarbon maturation within the basin vary considerably. Some maturation models favour hydrocarbon generation prior to cessation of Mesoproterozoic sedimentation (Crick et al., 1988; Dutkiewicz et al., 2007), others invoke Neoproterozoic hydrocarbon generation following deposition of the overlying Jamison sandstone (Taylor et al., 1994; Warren et al., 1998), while other models suggest peak hydrocarbon maturation in the Palaeozoic (Dutkiewicz et al., 2007; Faiz et al., 2021; RobSearch Australia, 1998; Taylor et al., 1994), or a combination thereof. Hence, the timing of hydrocarbon generation remains debated and is further clouded by a lack of independent basin low-temperature thermal history models, which must be addressed in order to advance understanding of the basin system.

A common thermochronological method applied to petroleum prospective basins is apatite fission track (AFT) analysis. The low closure temperature in the AFT system (ca. 120–60°C; Gleadow et al., 1986; Wagner & Van den Haute, 1992) is comparable with the oil window and, to a lesser extent, the gas window (oil window ≈ 120–50°C; gas window ≈ 150–120°C; Barker, 1989; Tissot et al., 1974; Waples, 1980), and is, therefore, a suitable method to investigate thermal events relevant to hydrocarbon generation. Crucially, inverse thermal history models generated using AFT data provide constraints on both the timing and magnitude of thermal events which are otherwise difficult to resolve. In this study, we present new AFT data from 20 sites within the McArthur Basin (Figure 1), using a combination of outcrop and sub-surface samples to provide the most spatially comprehensive published thermal history study of the basin to date. Inverse modelling (Gallagher, 2012) of the new thermochronological dataset was conducted for both surface and sub-surface samples which retained sufficient confined tracks for reliable inversion, and has been augmented by one-dimensional modelling of the thermal state of the basin in response to surficial heating by basaltic lavas to quantify the effect on AFT resetting.

Highlights

- Eruption of the Kalkarindji Large Igneous Province drove rapid heating across the McArthur Basin.
- Initial heating of shallow basin was short-lived but potentially linked to hydrocarbon maturation.
- Thickest preserved Kalkarindji lavas in the Beetaloo Sub-basin correlate with elevated hydrocarbon maturity.
- Cooled Kalkarindji lavas caused prolonged heating of underlying basin through thermal insulation.

2 | GEOLOGICAL BACKGROUND

2.1 | Basin history

The McArthur Basin is an extensive Palaeoproterozoic–Mesoproterozoic sedimentary basin exposed in the northern North Australian Craton, which unconformably overlies Palaeoproterozoic basement terranes of the Murphy Province, Arnhem Province and Pine Creek Orogen (e.g., Ahmad & Munson, 2013; Munson, 2016; Rawlings, 1999). Regional correlatives of the McArthur Basin have been proposed to the south of traditional basin exposure, in the Birrindudu Basin, Beetaloo Sub-Basin, South Nicholson Basin and Tomkinson Province that have led to the concept of a 'greater' McArthur

13652117, 2022, 6, Downloaded from https://onlinelibrary.wiley.com/doi/10.1111/bre.12691 by University of Adelaide Alumni, Wiley Online Library on [28/11/2022]. See the Terms and Conditions (https://onlinelibrary.wiley.com/terms-and-conditions) on Wiley Online Library for rules of use; OA articles are governed by the applicable Creative Commons License

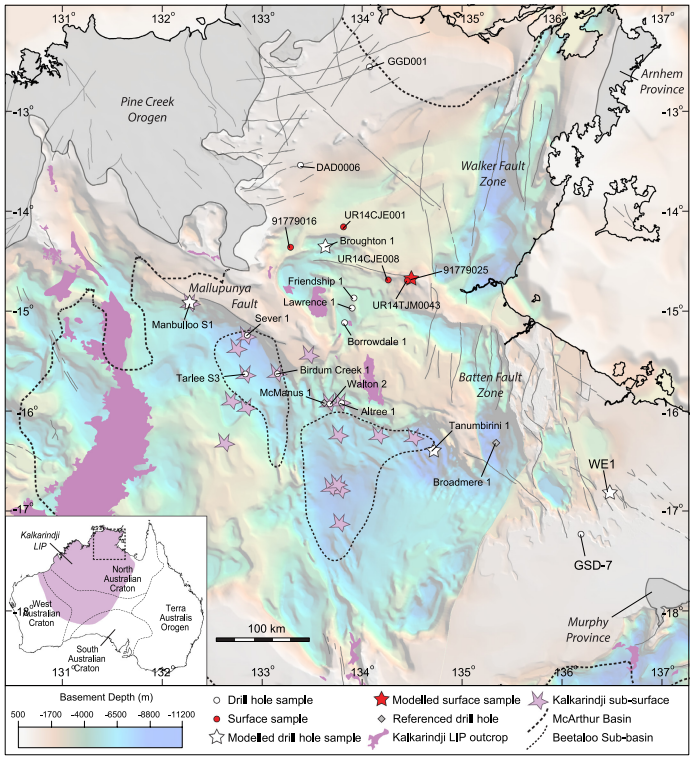

FIGURE 1 Sample locations collected for apatite fission track study within the McArthur Basin. Samples obtained at depth from drill-holes are shown in white, while outcrop samples are differentiated in red. The majority of samples did not provide sufficient data for robust thermal modelling, however, four wells and one outcrop sample that produced sufficient data for thermal history modelling are denoted by star symbols. Additional wells not analysed for AFT but discussed in text are shown for reference. The base of this overview is the SEEBASE depth to basement map showing depocentres and major structural highs (after Frogtech Geoscience, 2018). The overlain McArthur Basin extent includes the surface expression of McArthur sediments and the inferred sub-surface extent of strata from the Mesoproterozoic Wilton Package (Munson, 2016). The surface extent of the Kalkarindji LIP is complemented by occurrences of sub-surface Kalkarindji lavas intersected in drill holes. All latitudes and longitudes are given in the GDA94 system.

Basin (Close, 2014; Yang, Collins, Blades, et al., 2020), a current informal term for a regionally contiguous depositional system. The basin stratigraphy consists of five major unconformity-bounded depositional packages of sedimentary and minor volcanic rocks, deposited/erupted periodically between ca. 1820 and 1310 Ma, initially in a fluvial environment but transitioning to a dominantly shallow marine setting in later sequences (Ahmad & Munson, 2013; Rawlings, 1999; Yang, Collins, Cox, et al., 2020). The Wilton and Glyde Packages (ca. 1650–1400 Ma) in the upper McArthur Basin are of particular interest as they preserve organic carbon-rich black shales, and host significant hydrocarbon reserves derived from some of the oldest source rocks yet observed (Cox et al., 2016, 2022; Jackson et al., 1986). Source rocks within the basin have been identified as the Velkerri and Kyalla formations of the Roper Group within the Wilton Package, and the Barney Creek, Lynott and Yalko formations of the underlying McArthur Group of the Glyde Package (Crick et al., 1988; Jackson et al., 1988). Of these, the Velkerri and Barney Creek formations are considered the most prospective, preserving total organic carbon values up to 12% (e.g., Cox et al., 2022; Crick et al., 1988; Lanigan et al., 1994).

The youngest preserved sedimentation in the McArthur Basin is no younger than ca. 1310 Ma (Yang, Collins, Blades, et al., 2020; Yang, Collins, Cox, et al., 2020), after which the region is unconformably overlain by the Neoproterozoic Kiana Group of the Victoria Basin, including the Bukalara Sandstone and presently informally named Jamison sandstone (Anderson et al., 2019; Lanigan et al., 1994; Yang et al., 2018). The McArthur Basin region was then unconformably overlain by the Cambrian (ca. 510 Ma) Kalkarindji Large Igneous Province (LIP) lava flows (Ahmad & Munson, 2013; Evins et al., 2009; Glass & Phillips, 2006; Jourdan et al., 2014; Macdonald et al., 2005), which are infrequently preserved across the McArthur Basin (Figure 1). It is likely, however, that the lavas from the Kalkarindji LIP once extended across the majority of the basin prior to widespread erosion (Figure 1; Jourdan et al., 2014), with a maximum observed thickness of ca. 440 m within the basin (Hibbird, 1993b). There is, however, no observed evidence of sub-surface sills associated

13652117, 2022, 6, Downloaded from https://onlinelibrary.wiley.com/doi/10.1111/bre.12691 by University of Adelaide Alumni, Wiley Online Library on [28/11/2022]. See the Terms and Conditions (https://onlinelibrary.wiley.com/terms-and-conditions) on Wiley Online Library for rules of use; OA articles are governed by the applicable Creative Commons License

with the LIP intruding the McArthur region (Nixon, Glorie, Collins, Blades, et al., 2021). Extrusion of subaerial mafic lavas of the Kalkarindji LIP covered much of the western North Australian Craton and northern West Australian Craton, reaching maximum preserved thickness of ca. 1100 m in the West Australian Craton (Mory & Beere, 1988). In the North Australian Craton, the Kalkarindji volcanic sequences generally thin towards the east away from the probable eruption centre to the west, and overlie Proterozoic basement and sedimentary rocks (e.g., Ahmad & Munson, 2013; Glass & Phillips, 2006; Mory & Beere, 1988).

Sedimentary rocks of the Cryogenian–Devonian intra-cratonic Georgina Basin are present across much of northern Australia, and were deposited in terrestrial to shallow marine environments (e.g., Ahmad & Munson, 2013; Dunster et al., 2007; Walter et al., 1995). In the McArthur Basin, only Phanerozoic successions of the Georgina Basin are preserved, where Mid–Late Cambrian sequences unconformably overlie Kalkarindji lava flows or, where absent, Proterozoic rocks of the McArthur Basin or Kiana Group (Ahmad & Munson, 2013). Thickest sequences are preserved away from the McArthur Basin in the southern North Australian Craton, where Cambrian–Devonian rocks reach a maximum thickness of ca. 2.2 km (Smith et al., 2013), although many units observed in the southern Georgina Basin are absent in the McArthur Basin (Ahmad & Munson, 2013; Dunster et al., 2007). The McArthur and Georgina basins were subsequently unconformably overlain by the Jurassic–Cretaceous Carpentaria Basin (Abbott et al., 2001; Ahmad & Munson, 2013; Carson et al., 1999; Dunn, 1963; McConachie et al., 1990; Sweet et al., 1999), which thinly overlies much of the onshore North Australian Craton.

Following deposition of the Georgina Basin, the North Australian Craton was subject to prolonged deformation during the ca. 450–300 Ma Alice Springs Orogeny (e.g., Bradshaw & Evans, 1988; Hand et al., 1999; Mawby et al., 1999; Shaw & Black, 1991). Intracontinental orogenesis associated with north-south shortening and metamorphism expressed in the Amadeus Basin and Aileron and Irindina provinces (Haines et al., 2001; Shaw et al., 1992; Shaw & Black, 1991) is contemporaneous with large-scale structural disturbances and erosional events which extend far beyond the orogenic centre. Low-temperature cooling during the Alice Springs Orogeny is frequently observed in both basement (Boone et al., 2016; Glorie, Agostino, et al., 2017; Glorie et al., 2019; Hall et al., 2016, 2018; Nixon, Glorie, Collins, Whelan, et al., 2021; Quentin de Gromard et al., 2019; Reddy et al., 2015; Spikings et al., 2006) and basin (Tingate & Duddy, 2002; Wells, 1970) regions within both the North and South Australian cratons, implying the existence of a continental-scale thermal perturbation coincident with this event. The presence of widespread syn-deformational sedimentation has been observed across numerous central Australian basins (Haines et al., 2001), which demonstrates a complex deformational regime in which regions of uplift and erosion were spatially separated from contemporaneous siliciclastic deposition.

2.2 | Thermal history and maturation

Despite the high prospectivity for hydrocarbon exploration, the thermal and maturation history of the McArthur Basin remains poorly resolved. Hydrocarbon generation is generally considered to have occured as a response to burial in the Mesoproterozoic (Crick et al., 1988; Dutkiewicz et al., 2007), with earliest hydrocarbon generation proposed in the McArthur Group during maximum burial below McArthur and Nathan group sediments (ca. 1600 Ma; Kositcin et al., 2017; Rawlings, 1999), followed by later burial-related maturation in the Roper Group (ca. 1400–1300 Ma; Yang et al., 2018). Observations of linearly increasing hydrocarbon maturity below the Jamison sandstone suggest much of the hydrocarbon generation occurred prior to deposition of the Jamison sandstone (maximum depositional age of 959 ± 18 Ma; Yang et al., 2018), which overlies the source rocks in the McArthur Basin (Dutkiewicz et al., 2007; Taylor et al., 1994; Warren et al., 1998). While the Jamison sandstone provides a minimum constraint on Proterozoic hydrocarbon maturation, regional uplift and erosion associated with emplacement of the ca. 1330–1295 Ma Derim Derim Dolerite (Bodorkos et al., 2021; Nixon, Glorie, Collins, Blades, et al., 2021; Yang, Collins, Cox, et al., 2020) appears the most likely termination of sedimentation in the Mesoproterozoic. Today, preserved McArthur Basin stratigraphy exceeds thicknesses of 10 km in the major depocentre of the Beetaloo Sub-basin (Figure 1; Frogtech Geoscience, 2018), although this was likely even greater prior to erosion following Derim Derim Dolerite intrusion. In addition to burial-induced maturation models, some wells exhibit increasing hydrocarbon maturity proximal to the Derim Derim Dolerite sills, indicating that sill emplacement likely contributed to the thermal maturation of hydrocarbons (Crick et al., 1988; George & Ahmad, 2002; Taylor et al., 1994). While only intrusive sills of the Derim Derim Dolerite remain preserved, Crick et al. (1988) note that in some cases hydrocarbons mature upwards approaching the unconformity top of the Roper Group, suggesting the presence of now eroded surface lava flows in the Mesoproterozoic that further promoted thermal

13652117, 2022, 6, Downloaded from https://onlinelibrary.wiley.com/doi/10.1111/bre.12691 by University of Adelaide Alumni, Wiley Online Library on [28/11/2022]. See the Terms and Conditions (https://onlinelibrary.wiley.com/terms-and-conditions) on Wiley Online Library for rules of use; OA articles are governed by the applicable Creative Commons License

maturation. Such a scenario is consistent with an influx of juvenile material preserved in the Kyalla Formation of the upper Roper Group, which was likely sourced from the eroding mafic lava flows (Yang, Collins, Cox, et al., 2020).

While the majority of hydrocarbon maturation is presently attributed to a period of ca. 1400–950 Ma, prior to structural inversion and uplift within the McArthur Basin and deposition of the Jamison sandstone (Crick et al., 1988; Dutkiewicz et al., 2007; Taylor et al., 1994; Warren et al., 1998), a subsequent Palaeozoic maturation phase cannot be discounted. Strata of the Velkerri Formation in the Altree 2, McManus 1 and Walton 2 wells (Figure 1) were structurally offset by basin deformation following Jamison sandstone deposition, and demonstrate maturation profiles related to present-day offset depths (RobSearch Australia, 1998). This would suggest preserved hydrocarbons were generated in the Cambrian or later, after McArthur Basin structural inversion, a phenomenon also observed in the nearby Beetaloo Sub-basin (Faiz et al., 2021; Taylor et al., 1994). Unpublished AFT data referenced by Crick et al. (1988) suggest Roper Group sedimentary rocks emerged from the oil window (ca. 120–50°C) in the middle Palaeozoic, however, this is yet to be verified. A further published AFT study conducted on the Broadmere 1 well (Figure 1) in the eastern McArthur Basin (Duddy et al., 2004) predicts a complex Mesozoic thermal evolution. Duddy et al. (2004) propose cooling from >105°C between ca. 240–125 Ma, followed by a reheating peak of ca. 95–80°C in the Late Cretaceous, in response to deeper burial. In this model, subsequent cooling was facilitated by erosion of sedimentary overburden. These Mesozoic events have not been connected to any episodes of hydrocarbon generation within the basin, and do not appear to correlate with complementary deposition in adjacent basins.

3 | METHODS

3.1 | Sampling strategy

Samples were collected across the McArthur Basin from a combination of surface outcrop and drill hole material to provide both geographical and vertical resolution across the basin. A total of 19 drill core samples were taken from 15 wells within the McArthur Basin, including one of the deepest wells drilled in Australia at almost 4 km depth, Tanumbirini 1 (Table 1; Figure 1). Where possible, multiple samples were taken at different depths within the same well to capture thermal histories across a vertical profile, and modelled together to produce internally consistent models and better resolve the thermal evolution. Well samples were supplemented with an additional five outcrop samples to improve spatial coverage. Most sedimentary rocks in the Roper Group are notably deficient in detrital apatite, hence many samples have been collected from the ca. 1330–1295 Ma Derim Derim Dolerite sills, which intrude throughout the basin (Abbott et al., 2001; Bodorkos et al., 2021; Nixon, Glorie, Collins, Blades, et al., 2021; Yang, Collins, Cox, et al., 2020) and experienced a shared thermal history with the host sedimentary rocks following emplacement in the Mesoproterozoic. Additional samples were taken from McArthur Basin sedimentary rocks or Palaeoproterozoic crystalline basement, where available.

Apatite grains were liberated at the University of Adelaide using conventional crushing procedures, followed by panning, Frantz magnetic separation and immersion in liquid lithium heteropolytungstate (LST), diluted to specific gravity of 2.85 g/cm^3. Mounts were ground with #2000 silicon carbide paper to expose grain cores and polished with 3 and 1 µm diamond paste (e.g., Glorie, Alexandrov, et al., 2017), and subsequently etched with 5 M HNO_3 at 20 ± 0.5°C for 20 ± 0.5 s to reveal spontaneous fission tracks.

3.2 | Apatite fission track determination

Apatite grains were imaged with a Zeiss AXIO Imager M2m Autoscan microscope system prior to microprobe and laser analysis. Fission track densities and confined track lengths were manually identified using FastTracks v3.0.19 software, and samples were ground and repolished following laser ablation and irradiated with a ^{252}Cf source at the University of Adelaide for ca. 20 min and re-etched to reveal additional confined tracks for use in thermal modelling (Donelick & Miller, 1991).

3.3 | Electron probe micro analysis

Apatite major and minor elemental concentrations were determined by electron probe micro analysis (EPMA) at Adelaide Microscopy using a Cameca SXFive Electron Microprobe fitted with LTAP, PCO, LLIF and two LPET crystals. Analysis was conducted in a single stage analytical protocol with a 5 µm beam diameter at an accelerating voltage of 10 kV and beam current of 15 nA, using identical analytical conditions as in Nixon, Glorie, Collins, Whelan, et al. (2021). Full analytical parameters are provided in Appendix S1. Samples were analysed across two analytical

13652117, 2022, 6, Downloaded from https://onlinelibrary.wiley.com/doi/10.1111/bre.12691 by University of Adelaide Alumni, Wiley Online Library on [28/11/2022]. See the Terms and Conditions (https://onlinelibrary.wiley.com/terms-and-conditions) on Wiley Online Library for rules of use; OA articles are governed by the applicable Creative Commons License

TABLE 1 Locations and depth of McArthur Basin samples

Sample	Well	Unit	Lithology	Latitude	Longitude	Surface elevation (m)	Sample depth (m)
UR14CJE001	*Field sample*	Derim Derim Dolerite	Dolerite	−14.1638	133.8054	133	0
UR14CJE008	*Field sample*	Derim Derim Dolerite	Dolerite	−14.6935	134.2541	99	0
UR14TJM0043	*Field sample*	Derim Derim Dolerite	Dolerite	−14.7017	134.4432	20	0
91779016	*Field sample*	West Branch Volcanics	Rhyolite	−14.3673	133.2791	198	0
91779025	*Field sample*	Urapunga Granite	Granite	−14.6885	134.4829	19	0
La1-1	Lawrence 1	Derim Derim Dolerite	Dolerite	−14.9758	133.8918	106	204.65–206.82
Fri1-1	Friendship 1	Derim Derim Dolerite	Dolerite	−14.8744	133.9112	62	304.60–306.59
GSD07-01	GSD-7	Sly Creek Sandstone	Sandstone	−17.2356	136.1785	226	384.30–384.50
GGD001-04	GGD001	Mamadawerre Sandstone	Sandstone	−12.5656	134.0664	91	461.90–462.44
TMB-3	Tanumbirini 1	Bukalara Sandstone	Sandstone	−16.3991	134.7038	210	480.00–580.00
TMB-6	Tanumbirini 1	Bukalorkmi Sandstone	Sandstone	−16.3991	134.7038	210	1205.00–1295.00
TMB-10	Tanumbirini 1	Moroak Sandstone	Sandstone	−16.3991	134.7038	210	2080.00–2180.00
Bor2-1	Borrowdale 1	Derim Derim Dolerite	Dolerite	−15.1217	133.81670	128	489.26–491.68
We1-03	WE1	Masterton Sandstone	Sandstone	−16.8196	136.4671	136	590.00–590.50
We1-07	WE1	Masterton Sandstone	Sandstone	−16.8196	136.4671	136	808.90–809.35
Br-12	Broughton 1	Katherine River Group	Sandstone	−14.3600	133.6261	110	692.00–692.51
Br-09	Broughton 1	Katherine River Group	Sandstone	−14.3600	133.6261	110	865.90–866.53
Mb1-1	Manbulloo S1	Fraynes Formation	Tuff	−14.9277	132.2684	149	758.90–758.95
Sv1-1	Sever 1	Derim Derim Dolerite	Dolerite	−15.2465	132.8440	175	800.64–802.54
Wal2-2	Walton 2	Derim Derim Dolerite	Dolerite	−15.9319	133.6679	204	911.08–913.41
DAD6-1	DAD0006	Oenpelli Dolerite	Dolerite	−13.5476	133.3761	382	1139.86–1143.00
BC1-4	Birdum Creek 1	Derim Derim Dolerite	Dolerite	−15.6305	133.1444	182	1445.00–1475.00
TS3-1	Tarlee S3	Derim Derim Dolerite	Dolerite	−15.6324	132.8260	191	1508.93–1511.29
Alt2-1	Altree 1	Derim Derim Dolerite	Dolerite	−15.9236	133.7866	216	1696.39–1698.72

Note: All coordinates are provided in the GDA94 system. Surface Elevation is the point elevation of surface following the Global Multi-resolution Terrain Elevation Data (GMTED) topographic imagery (Danielson & Gesch, 2011), while Sample Depth is the depth from which samples were taken below this point.

13652117, 2022, 6, Downloaded from https://onlinelibrary.wiley.com/doi/10.1111/bre.12691 by University of Adelaide Alumni, Wiley Online Library on [28/11/2022]. See the Terms and Conditions (https://onlinelibrary.wiley.com/terms-and-conditions) on Wiley Online Library for rules of use; OA articles are governed by the applicable Creative Commons License

sessions (sessions EPMA-19 and EPMA-21). Durango apatite was interspaced within analytical sequences and served as an accuracy standard (Chew et al., 2016; Marks et al., 2012).

3.4 | LA-ICP-MS analysis

Uranium and other trace element concentrations were acquired by LA-ICP-MS using a RESOlution LR 193 nm excimer laser connected to an Agilent 7900x ICP-MS at Adelaide Microscopy. Full analytical parameters are provided in Appendix S1. Durango apatite was interspaced as a secondary standard throughout analytical sessions to ensure quality of data (Chew et al., 2016). Data collection was performed in five analytical sessions (sessions LA-17, LA-18, LA-19a, LA-19b and LA-20). Geochemical data were reduced using the 'X_Trace_Elements_IS' data reduction package of Iolite v3.32 software (Paton et al., 2011), using NIST610 as the primary standard (Jochum et al., 2011).

3.5 | Apatite fission track age calculation

Fission track ages were calculated using the LA-ICP-MS method (Hasebe et al., 2004, 2013; Vermeesch, 2017), using ^{238}U concentrations and fission track densities to calculate single grain ages. Single grain and population central ages were calculated using IsoplotR software (Vermeesch, 2018) and calibrated to a session-specific Zeta calculated from parallel analysis of a Durango apatite standard (Vermeesch, 2017).

3.6 | Thermal history modelling

Thermal history modelling was undertaken with QTQt software (Gallagher, 2012), using inputs of AFT single grains ages, confined track length distributions, and using chlorine concentration as the kinetic parameter (Green et al., 1986). No c-axis projection was applied for confined tracks in modelling or track length profiling. Mapped and sub-surface geology was also considered and included as model constraints to further refine the reconstructions (e.g., Green & Duddy, 2021). Unconformable contacts between stacked basins and volcanics provide a means to constrain sample depth immediately preceding deposition of an overlying unit, and allow for inference of sample palaeotemperature during thermal history modelling, assuming an undisturbed thermal gradient. During inverse thermal modelling, sample temperatures were constrained to calculated palaeotemperatures at unconformities prior to emplacement and deposition of the Kalkarindji lava flows, and sediments of the Georgina and Carpentaria basins, following the stratigraphy outlined in Figure 2

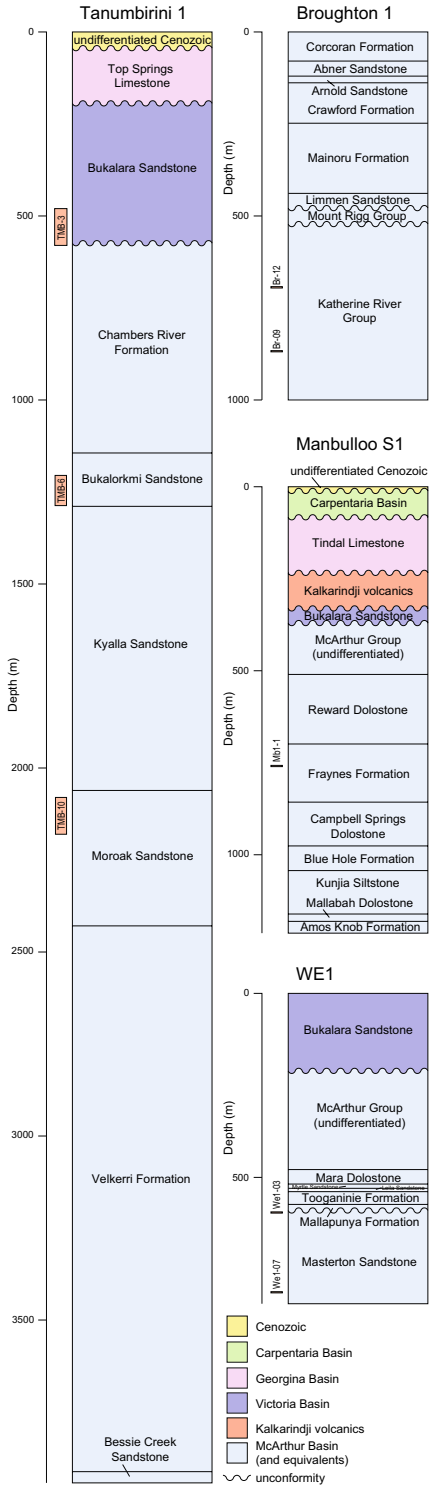

FIGURE 2 Stratigraphy of modelled thermal history wells in the McArthur Basin following Allison and Sheehan (1982), Torkington and Ledlie (1988), Adderly (2015) and Pangaea Resources (2015b). Depth intervals of samples used for AFT modelling are provided to the left of each stratigraphic column.

13652117, 2022, 6, Downloaded from https://onlinelibrary.wiley.com/doi/10.1111/bre.12691 by University of Adelaide Alumni, Wiley Online Library on [28/11/2022]. See the Terms and Conditions (https://onlinelibrary.wiley.com/terms-and-conditions) on Wiley Online Library for rules of use; OA articles are governed by the applicable Creative Commons License

(Adderly, 2015; Allison & Sheehan, 1982; Pangaea Resources, 2015b; Torkington & Ledlie, 1988). Where these units are absent, their position was inferred using local geology to ensure reconstructions are produced using consistent prior constraints. Extended modelling rationale and derivation of constraints, as well as modelling outcomes using only unconformable horizons in each well, are provided in Appendix S1, following the recommendations by Flowers et al. (2015).

3.7 | One-dimensional thermal modelling

One-dimensional thermal modelling was undertaken for the McArthur Basin following the eruption of the Kalkarindji LIP, using the Tectotherm program by Hasterok et al. (in prep.), available at https://github.com/dhasterok/tectotherm. This program simulates tectonomagmatic scenarios with user-defined sedimentation and erosion history. TectoTherm solves the one-dimensional heat conduction equation using the Crank-Nicholson finite difference method. The boundary conditions are set to a fixed surface temperature of 25°C, consistent with the position of the North Australian Craton at equatorial latitudes during the Cambrian (Merdith et al., 2021) during a period of relatively elevated global surface temperatures (Hearing et al., 2018; Wotte et al., 2019), with a user-defined heat flow at the base of the lithosphere (30 m/Wm^2). The initial geotherm is computed as a steady-state geotherm computed in a manner similar to Chapman (1986) with pressure and temperature-dependent physical properties. We selected a depth node spacing of 0.1 km and a time step of 0.001 million years, using thermal properties of sandstone and shale lithologies in the upper 10 km of the crust overlying crystalline basement and mantle rocks (detailed in Appendix S1). TectoTherm replaces rock types with physical properties provided in a database drawn from published measurements and average physical properties computed from a global geochemical dataset (Gard et al., 2019). The physical properties are adjusted for temperature and pressure effects as the model evolves. To simulate a volcanic flow, models were run in which volcanic layers with thickness of 0.5, 0.75 and 1 km were added to the top of the model at a melt temperature of 1000°C. The temperatures at the top and bottom of the lava flow are smoothed slightly (a distance ±1/8 of the flow thickness) to reduce numerical artefacts while reducing the cooling time only slightly. The high-resolution models were to run for a modelling time of 2 million years, while additional models were run for each thickness at a depth node spacing of 0.1 km and a time step of 0.02 million years over a simulation time of 5 million years to model the steady-state conditions of the basin after lavas had completely cooled.

4 | OBSERVATIONS AND RESULTS

4.1 | Geochemistry

4.1.1 | Data accuracy

Durango apatite was analysed as a secondary standard to confirm data reliability and monitor possible instrument drift. Durango apatite returned weighted mean chlorine abundances of 0.43 ± 0.01 wt% (Session EPMA-19) and 0.37 ± 0.01 wt% (Session EPMA-21) in different crystals in each session, and no obvious drift was observed between sessions. Chlorine weighted mean plots for Durango secondary standards are provided in Appendix S1. The measured range of Durango apatite chlorine concentrations across analytical sessions is consistent with published concentrations of ca. 0.46–0.37 wt% (Chew et al., 2016), suggesting chlorine data from these sessions are reliable. The full standard elemental dataset is provided in Appendix S2.

4.1.2 | Geochemistry results

Apatites from sampled McArthur Basin sedimentary and igneous rocks display a dominantly fluorapatite chemistry. Average chlorine concentrations are relatively low in all samples, ranging between 0.51 and 0.04 wt%, biased slightly higher towards apatites sourced from dolerites. Furthermore, intra-sample chlorine variations are minor (Figure 3), and do not exhibit a clear correlation with single-grain AFT ages.

4.2 | Apatite fission track data

4.2.1 | Data accuracy

Single-grain AFT ages were calibrated using a session-specific Zeta factor based on Durango apatite AFT data, following Vermeesch (2017). Analysed Durango apatite returned weighted mean AFT ages of 30.9 ± 4.3 Ma (Session LA-17), 31.3 ± 2.1 Ma (Session LA-18), 32.8 ± 5.2 Ma (Session LA-19a), 30.0 ± 1.6 Ma (Session LA-19b) and 28.1 ± 4.8 Ma (Session LA-20), all of which are within uncertainty of the published standard ^{40}Ar/^{39}Ar age (31.44 ± 0.18 Ma; McDowell et al., 2005). Younger standards such as Durango can sometimes have the effect of propagating larger than expected errors to older geological

13652117, 2022, 6, Downloaded from https://onlinelibrary.wiley.com/doi/10.1111/bre.12691 by University of Adelaide Alumni, Wiley Online Library on [28/11/2022]. See the Terms and Conditions (https://onlinelibrary.wiley.com/terms-and-conditions) on Wiley Online Library for rules of use; OA articles are governed by the applicable Creative Commons License

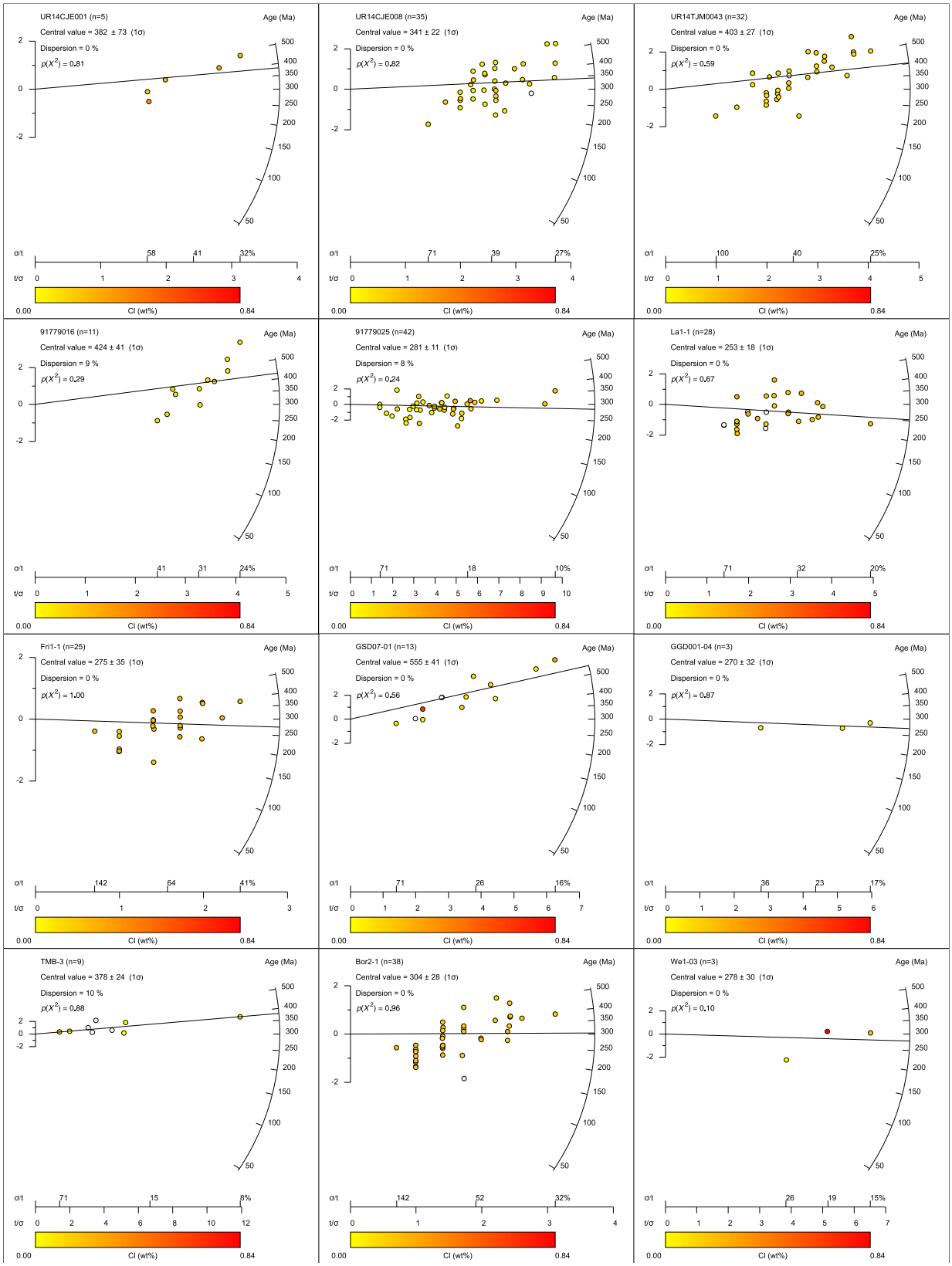

FIGURE 3 AFT radial plots for the McArthur Basin samples, with a single statistically identified age population (central age) calculated for each sample (Vermeesch, 2018). Single-grain ages are coloured by EPMA derived Cl content. $p(\chi^2)$ denotes the chi-square value for the central age population.

13652117, 2022, 6, Downloaded from https://onlinelibrary.wiley.com/doi/10.1111/bre.12691 by University of Adelaide Alumni, Wiley Online Library on [28/11/2022]. See the Terms and Conditions (https://onlinelibrary.wiley.com/terms-and-conditions) on Wiley Online Library for rules of use; OA articles are governed by the applicable Creative Commons License

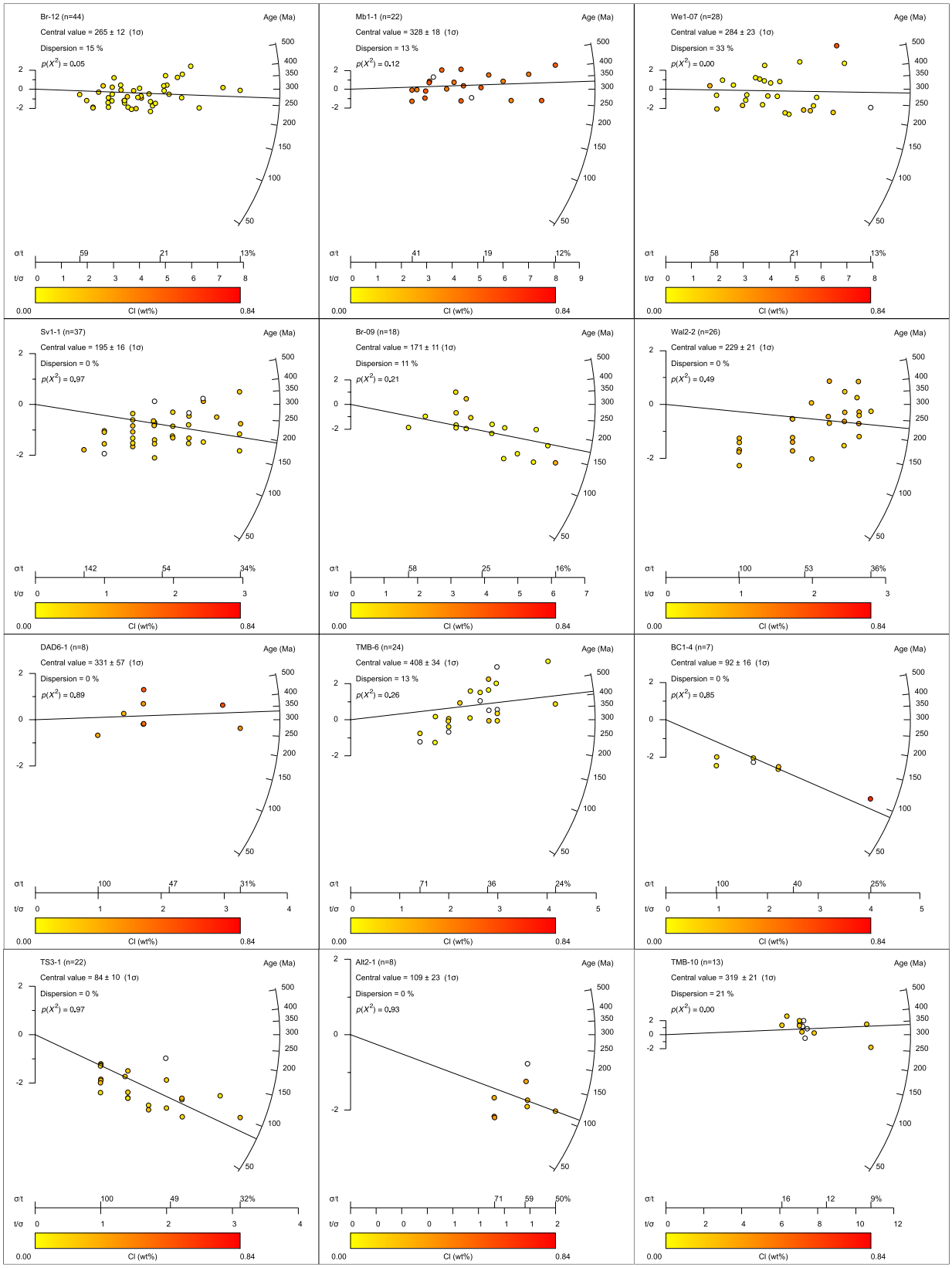

FIGURE 3 (Continued)

13652117, 2022, 6, Downloaded from https://onlinelibrary.wiley.com/doi/10.1111/bre.12691 by University of Adelaide Alumni, Wiley Online Library on [28/11/2022]. See the Terms and Conditions (https://onlinelibrary.wiley.com/terms-and-conditions) on Wiley Online Library for rules of use; OA articles are governed by the applicable Creative Commons License

samples, although should not meaningfully skew the calculated age so data are nevertheless considered reliable. The full standard elemental dataset is provided in Appendix S2.

4.2.2 | Apatite fission track results

Radial plots exhibit low single-grain age-dispersion and no significant age variation corresponding to chemistry (Figure 3), and do not display 'open-jaw' age characteristics (O'Sullivan & Parrish, 1995). Although two samples do fail the chi-square test (We1-07 and TMB-10), this test has often been found unsuitable for use more precise AFT age determinations on old, high U bearing apatites such as these by LA–ICP–MS methodology (McDannell, 2020), and coupled with the lack of 'open-jaw' spread it is concluded all samples reveal a single, central age population, which range from 555 to 84 Ma (Table 2; Figure 3). Due to the low number of apatite grains and commonly small grain sizes, particularly in dolerite samples, only six samples yielded sufficient confined tracks (>60) for confident interpretation. For these samples, confined track distributions are unimodal with broad, weakly negatively skewed distributions, with the exception of sample TMB-6, which exhibits a positively skewed distribution (Figure 4). Mean track lengths (MTL) generally decrease with increasing depth, from 12.2 ± 1.4 μm at the surface to 10.2 ± 1.7 μm at ca. 2180 m depth (Table 2).

The samples exhibit progressively decreasing AFT central ages with increasing depth and temperature (Figure 5), consistent with the current geothermal gradient of ca. 35–30°C/km. These trends, however, show disparity across different regions of the basin. The youngest ages are consistently retained in what can broadly be termed the central McArthur Basin (Figure 5), as well as the northernmost sample, taken proximal to north-south striking faults (GGD001; Figure 1). Samples from this group preserve AFT central ages between 403 ± 27 Ma and 281 ± 11 Ma at the surface, decreasing to 109 ± 23 Ma in the deepest sample at ca. 1700 m depth. Moderately older ages are preserved in the northwestern McArthur Basin that overlies shallower basement bordering the Pine Creek Orogen (Figures 1 and 5), and preserve AFT central ages of 424 ± 41 Ma at the surface to 331 ± 57 Ma in the deepest sample at ca. 1140 m. Samples from the Tanumbirini 1 well, in one of the deepest regions of the McArthur Basin (Figure 1), yield surprisingly little decrease in AFT ages with depth, with ages varying between 408 ± 34 Ma and 319 ± 21 Ma across a depth range of ca. 2180–480 m (Figure 5). The oldest preserved central age of 555 ± 41 Ma was obtained from a depth of ca. 384 m in the GSD7 well, which overlies shallow basement in the southeastern McArthur Basin (Figures 1 and 5).

While McArthur Basin sedimentary rocks were deposited in the Palaeoproterozoic–Mesoproterozoic, preserved AFT ages are exclusively Palaeozoic–Mesozoic in age, and hence do not allow for investigation of the low-temperature history prior to the Phanerozoic. Thermal history models are displayed in Figure 6, with individual model variants and residuals provided in Appendix S1. No models yield sufficient data for robust determination of the palaeogeothermal gradient required for estimation of palaeotemperatures across a vertical profile away from sampled strata, hence the timing of thermal events has been emphasised over absolute temperatures experienced in the region. Thermal history models for the Broughton 1 and WE1 wells and the 91779025 outcrop sample demonstrate similar, yet complex, thermal histories. Modelling predicts heating of sediments during emplacement of the Kalkarindji LIP at ca. 510 Ma, and continuing following burial below the Georgina Basin. Subsequent slow cooling initiated at ca. 390 Ma. While unable to be thermally modelled, AFT central ages for samples in the central McArthur Basin are similar to those of modelled samples from Broughton 1, WE1 and 91779025 (Table 2; Figure 5), consistent with comparable thermal histories for samples in this region. A similar thermal history is also predicted for the Manbulloo S1 well in the northwestern McArthur Basin, however, more rapid cooling is observed at ca. 390–360 Ma, which is not observed for the central McArthur samples (Figure 6). The northwestern McArthur Basin samples DAD6-1 and 91779016 preserve older AFT central ages than observed for central McArthur Basin samples, as does sample Mb1-1, which further indicates that the northwestern samples share comparable thermal histories to each other.

The Tanumbirini 1 well preserves a significantly different Palaeozoic thermal history than observed elsewhere in the McArthur Basin (Figure 6). The Tanumbirini 1 model reveals rapid and intense heating immediately after the eruption of the ca. 510 Ma Kalkarindji Province, which was followed quickly by a thermal rebound to pre-heating temperatures. Devonian–Carboniferous cooling recognised in other McArthur Basin wells appears absent in Tanumbirini 1, indicating this well was not exposed to a significant thermal event after cooling from the Cambrian thermal maximum.

4.3 | One-dimensional thermal modelling

One-dimensional modelling of the thermal response to basaltic lavas emplaced on the surface of the McArthur Basin was used to test the hypothesis of Kalkarindji flows imparting sufficient heating to disturb fission track retention

13652117, 2022, 6, Downloaded from https://onlinelibrary.wiley.com/doi/10.1111/bre.12691 by University of Adelaide Alumni, Wiley Online Library on [28/11/2022]. See the Terms and Conditions (https://onlinelibrary.wiley.com/terms-and-conditions) on Wiley Online Library for rules of use; OA articles are governed by the applicable Creative Commons License

TABLE 2 Summary of AFT results, separated into regions as shown in Figure 5

	Sample	Depth (m)	ρ_s ($\times 10^6$/cm^2)	N_s	n	$^{238}U \pm 1\sigma$ (ppm)	Cl (wt%)	C. Age (Ma)	$p(\chi^2)$	Disp (%)	n_l	MTL $\pm$ 1 SD (μm)
Central McArthur Basin	UR14CJE001	0	0.72	28	5	3.68 $\pm$ 0.19	0.25	382 $\pm$ 73	0.81	0	–	–
	UR14CJE008	0	0.66	254	35	3.89 $\pm$ 0.17	0.09	341 $\pm$ 22	0.82	0	–	–
	UR14TJM0043	0	0.69	232	32	3.41 $\pm$ 0.16	0.13	403 $\pm$ 27	0.59	0	–	–
	91779025	0	2.29	888	42	16.41 $\pm$ 0.45	0.08	281 $\pm$ 11	0.24	8	224	12.2 $\pm$ 1.4
	La1-1	204.65–206.82	0.51	215	28	3.76 $\pm$ 0.16	0.21	253 $\pm$ 18	0.67	0	–	–
	Fri1-1	304.60–306.59	0.51	61	25	3.66 $\pm$ 0.24	0.22	275 $\pm$ 35	1.00	0	–	–
	GGD001-04	461.90–462.44	3.48	75	3	29.23 $\pm$ 1.57	0.04	270 $\pm$ 32	0.87	0	–	–
	Bor2-1	489.26–491.68	0.52	118	38	3.44 $\pm$ 0.23	0.18	304 $\pm$ 28	0.96	0	–	–
	We1-03	590.00–590.50	3.38	89	3	32.31 $\pm$ 1.30	0.35	278 $\pm$ 30	0.10	0	–	–
	Br-12	692.00–692.51	1.61	817	44	15.48 $\pm$ 0.62	0.06	265 $\pm$ 12	0.05	15	123	11.4 $\pm$ 1.4
	We1-07	808.90–809.35	2.84	607	28	26.08 $\pm$ 0.89	0.09	284 $\pm$ 23	0.00	33	61	11.5 $\pm$ 1.4
	Sv1-1	800.64–802.54	0.33	144	37	3.51 $\pm$ 0.15	0.16	195 $\pm$ 16	0.97	0	–	–
	Br-09	865.90–866.53	1.41	324	18	21.20 $\pm$ 0.80	0.05	171 $\pm$ 11	0.21	11	–	–
	Wal2-2	911.08–913.41	0.36	117	26	3.40 $\pm$ 0.15	0.22	229 $\pm$ 21	0.49	0	–	–
	BC1-4	1445.00–1475.00	0.17	35	7	3.34 $\pm$ 0.13	0.22	92 $\pm$ 16	0.85	0	–	–
	TS3-1	1508.93–1511.29	0.22	68	22	5.69 $\pm$ 0.29	0.17	84 $\pm$ 10	0.97	0	–	–
	Alt2-1	1696.39–1698.72	0.35	22	8	7.03 $\pm$ 0.28	0.29	109 $\pm$ 23	0.93	0	–	–
Northwestern McArthur Basin	91779016	0	0.55	123	11	2.55 $\pm$ 0.11	0.09	424 $\pm$ 41	0.29	9	–	–
	Mb1-1	758.90–758.95	1.24	549	22	7.00 $\pm$ 0.24	0.51	328 $\pm$ 18	0.12	13	274	12.2 $\pm$ 1.7
	DAD6-1	1139.86–1143.00	0.72	35	8	3.61 $\pm$ 0.22	0.41	331 $\pm$ 57	0.89	0	–	–
Tanumbirini 1	TMB-3	480.00–580.00	2.76	270	9	10.88 $\pm$ 0.64	0.05	378 $\pm$ 24	0.88	10	–	–
	TMB-6	1205.00–1295.00	0.92	169	24	4.95 $\pm$ 0.36	0.10	408 $\pm$ 34	0.26	13	77	11.5 $\pm$ 1.5
	TMB-10	2080.00–2180.00	3.79	825	13	21.17 $\pm$ 1.14	0.17	319 $\pm$ 21	0.00	21	90	10.2 $\pm$ 1.7
Southeastern McArthur Basin	GSD07-01	384.30–384.50	2.57	189	13	11.42 $\pm$ 0.62	0.16	555 $\pm$ 41	0.56	0	–	–

Note: ρ_s is the average surface density of spontaneous fission tracks. N_s is the total number of spontaneous fission tracks counted in the sample. n is the number of grains analysed in the sample. ^{238}U is the average concentration of uranium–238 for all grains in the sample, with uncertainty given as 1σ. C. Age is the sample AFT central age as calculated using IsoplotR software (Vermeesch, 2018), where all errors represent 1σ. $p(\chi^2)$ is the chi-square probability that all grains in the population may be attributed to a single age population. Disp. is the percentage of dispersion within the sample AFT ages. n_l is the number of confined tracks measured for all grains of the sample. MTL is the mean confined track length, with uncertainty quoted as 1 standard deviation.

13652117, 2022, 6, Downloaded from https://onlinelibrary.wiley.com/doi/10.1111/bre.12691 by University of Adelaide Alumni, Wiley Online Library on [28/11/2022]. See the Terms and Conditions (https://onlinelibrary.wiley.com/terms-and-conditions) on Wiley Online Library for rules of use; OA articles are governed by the applicable Creative Commons License

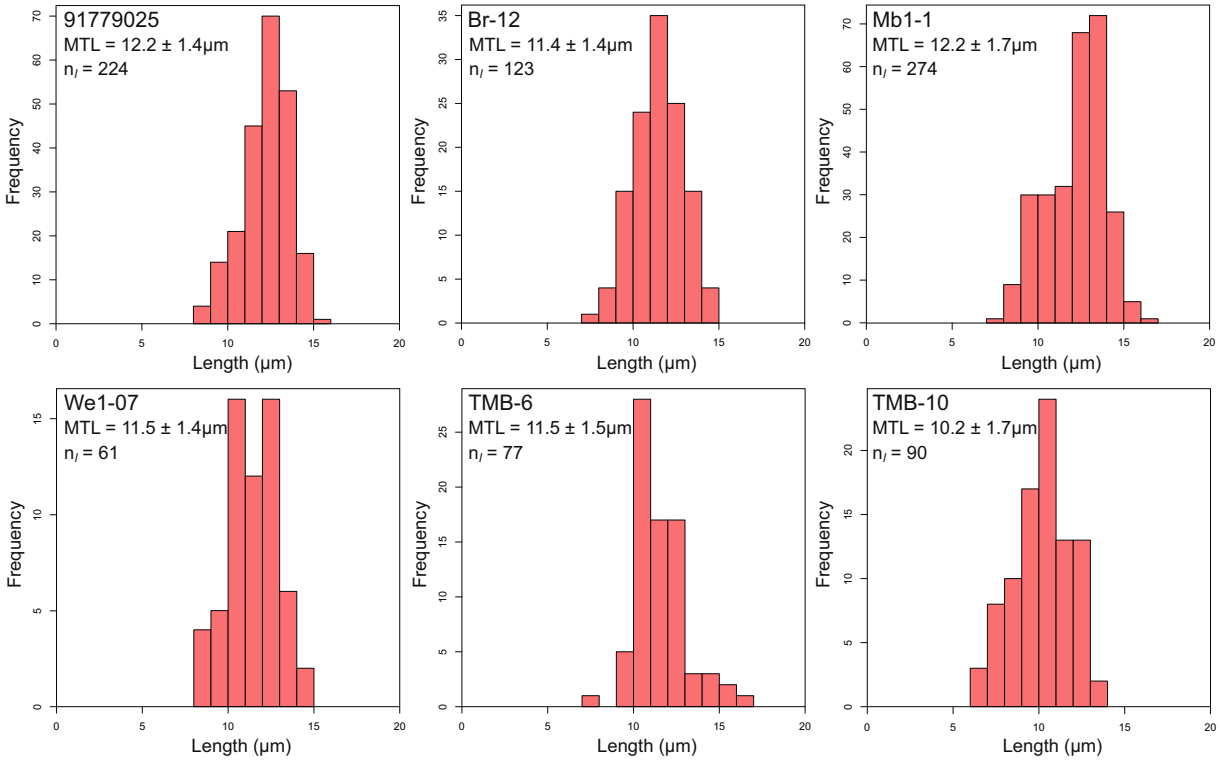

FIGURE 4 Confined fission track histograms for all McArthur Basin samples yielding sufficient confined tracks (>60) for interpretation. MTL is the mean confined track length for each sample and associated 1σ uncertainty. n_l is the number of confined track lengths in each sample.

(Figure 7). Presently, the most extensive Kalkarindji flows within the McArthur Basin reach a thickness ca. 440 m (Hibbird, 1993b), and reach a maximum preserved thickness of ca. 1100 m in the West Australian Craton (Mory & Beere, 1988). It is likely, however, that significant thicknesses of Kalkarindji lavas have been eroded since emplacement, as evidenced by the presence of a regional erosional unconformity across the upper surface of the flows (Ahmad & Munson, 2013; Kruse et al., 1994), making it difficult to resolve the original volume of extruded lava. Because the original thickness of extruded lava is uncertain, we consider multiple scenarios with an original thicknesses of 500 m (scenario 1), 750 m (scenario 2) and 1000 m (scenario 3). Based on these models, all thicknesses of lava would have caused significant heating of the shallow basin (Figure 7) and rapid resetting of AFT ages over a time span of thousands of years in the upper ca. 1 km (scenario 1) to ca. 2 km (scenario 3). The models further predict that the magmatic-induced high-magnitude, shallow dispersion heating subsequently transitioned to a new steady-state geothermal gradient, which in moderate scenarios elevated the temperature of the sub-surface basin sediments by ca. 24°C in scenario 1 (500 m lava eruption) and ca. 33°C in scenario 2 (750 m lava eruption) due to insulation by low thermal conductivity basalts (Gard et al., 2019). In a more extreme scenario of 1000 m of lava extrusion sediments were predicted to experience heating by additional ca. 47°C (scenario 3). These elevated temperatures were maintained until the Kalkarindji basalts and any subsequent Georgina Basin overburden was removed, likely persisting long enough to anneal the AFT system in the more conventional partial annealing zone of ca. 120–60°C over millions of years (Gleadow et al., 1986; Laslett et al., 1987; Wagner & Van den Haute, 1992).

5 | DISCUSSION

5.1 | Kalkarindji volcanism

The thermal history models from this study reveal heating in the basin coincident with LIP volcanism, which is most rapid in the Tanumbirini 1 well (Figure 6), and is likely also responsible for AFT resetting in the GSD-7 well in the east of the basin (Figure 5). Hence, we interpret the abrupt heating as a response to the Kalkarindji event, during which time the basin was overlain by thick lava flows coinciding with regional lithospheric thinning (Glass, 2002). Deposition of Georgina Basin sediments followed extrusion of Kalkarindji lavas in the McArthur Basin, further insulating the sub-surface and preventing rapid thermal rebound across most of the basin. Thermal

13652117, 2022, 6, Downloaded from https://onlinelibrary.wiley.com/doi/10.1111/bre.12691 by University of Adelaide Alumni, Wiley Online Library on [28/11/2022]. See the Terms and Conditions (https://onlinelibrary.wiley.com/terms-and-conditions) on Wiley Online Library for rules of use; OA articles are governed by the applicable Creative Commons License

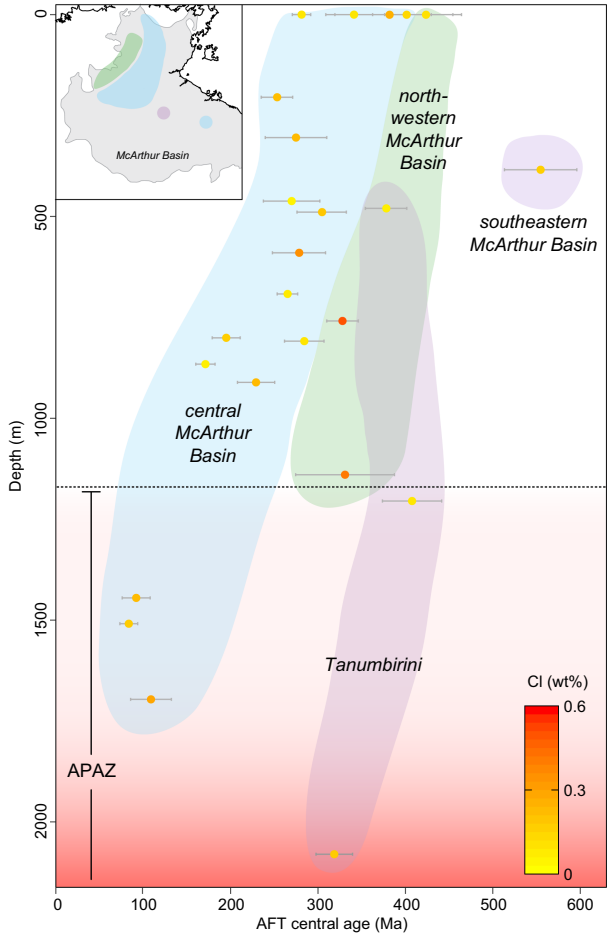

FIGURE 5 Plot of AFT central ages and associated 1σ uncertainty of McArthur Basin samples against depth below surface, coloured by average sample Cl content. AFT central ages typically decrease with depth, due to temperature increase with depth following the geothermal gradient. Samples have been grouped to geographical regions of the 'central McArthur Basin', 'northwestern McArthur Basin', 'Tanumbirini' and 'southeastern McArthur Basin' as shown in inset, and demonstrate different AFT versus depth trends between these regions.

rebound is observed, however, in Tanumbirini 1 proximal to the Beetaloo Sub-basin, suggesting only minor Palaeozoic sedimentation occurred in this region following Kalkarindji magmatism, where presently Georgina Basin sediments are only ca. 150 m thick (Adderly, 2015).

The heating event observed in the QTQt models for the Tanumbirini 1 well is coincident with extrusion of the Kalkarindji LIP (Figure 6) and consistent with heating below ca. 750 m of Kalkarindji flood basalts (Figure 7). Such volumes of lava would have rapidly heated the upper ca. 2 km of this vertical sequence and reset AFT sample TMB-3 at temperatures >240°C maintained for 10,000 years, and TMB-6 at temperatures >140°C for 30,000 years (Laslett et al., 1987). In this scenario, sample TMB-10 did not experience the short-lived elevated temperatures reached at shallower samples, with the AFT system instead reset at temperatures of ca. 105°C reached during subsequent steady-state conditions caused by insulation by cooled basaltic lavas (Figure 7). This different mechanism of heating and partial reset may at least partially explain the anomalously older AFT age preserved by this sample (Figure 5). Basaltic overburden in this region must have subsequently been removed in the following 20 million years, prior to deposition of the overlying Top Springs Limestone (Figure 2; Ahmad & Munson, 2013; Dunster et al., 2007). A similar scenario is predicted in the southeastern McArthur Basin, where sample GSD07-01 preserves an AFT age of 555 ± 41 Ma, overlapping with the age of the Kalkarindji eruption. This shallow sample would have been totally reset by sub-surface heating from ca. 500 m of lava flows and does not record subsequent insulation-driven long-term heating and associated AFT annealing (Figure 7), and likely defines a minimum easterly extent of the Kalkarindji LIP. Conversely, the Manbulloo S1, Broughton 1 and WE1 wells in the central and northwestern McArthur Basin display a more prolonged heating event in their thermal history models, which initiated during Kalkarindji emplacement and persisted throughout the Cambrian to Devonian (Figure 6). Both basalts of the Kalkarindji LIP and relatively unconsolidated sediments of the Georgina Basin possess very low thermal conductivities (Gard et al., 2019), and would thus have served as effective thermal insulators of the underlying basin. This protracted residence at elevated temperatures is, therefore, more consistent with insulation by low thermal conductivity basalts and sediments of the Georgina Basin (Ahmad & Munson, 2013; Kruse et al., 1994; Kruse & Radke, 2008), rather than short-lived heating observed in the Tanumbirini well. This region might have been covered by thinner lava flows than observed around Tanumbirini 1 (Figure 7), however, burial below the Georgina sediments allowed these flows to be preserved for longer thus resetting samples at lower temperature due to prolonged residence at these temperatures (Figure 7).

Preserved Kalkarindji lava flows are notably thicker in the central Beetaloo Sub-basin than elsewhere in the McArthur Basin (Figure 8a; Markov et al., 2021), evidenced most strikingly in the Chanin 1, Ronald 1 and Burdo 1 wells, which intersect preserved basaltic packages of 440–270 m thickness (Hibbird, 1993a, 1993b; Menpes, 1993). While the presence of a basin-wide erosional unconformity at the upper surface of the Kalkarindji LIP (Ahmad & Munson, 2013; Kruse et al., 1994) makes accurate estimation of regional lava thicknesses problematic, observation of greater volumes of lava in the Beetaloo Sub-basin is consistent with more pronounced thermal and hydrocarbon maturation trends within the sub-basin. The significant heating pulse observed in the Tanumbirini 1

13652117, 2022, 6, Downloaded from https://onlinelibrary.wiley.com/doi/10.1111/bre.12691 by University of Adelaide Alumni, Wiley Online Library on [28/11/2022]. See the Terms and Conditions (https://onlinelibrary.wiley.com/terms-and-conditions) on Wiley Online Library for rules of use; OA articles are governed by the applicable Creative Commons License

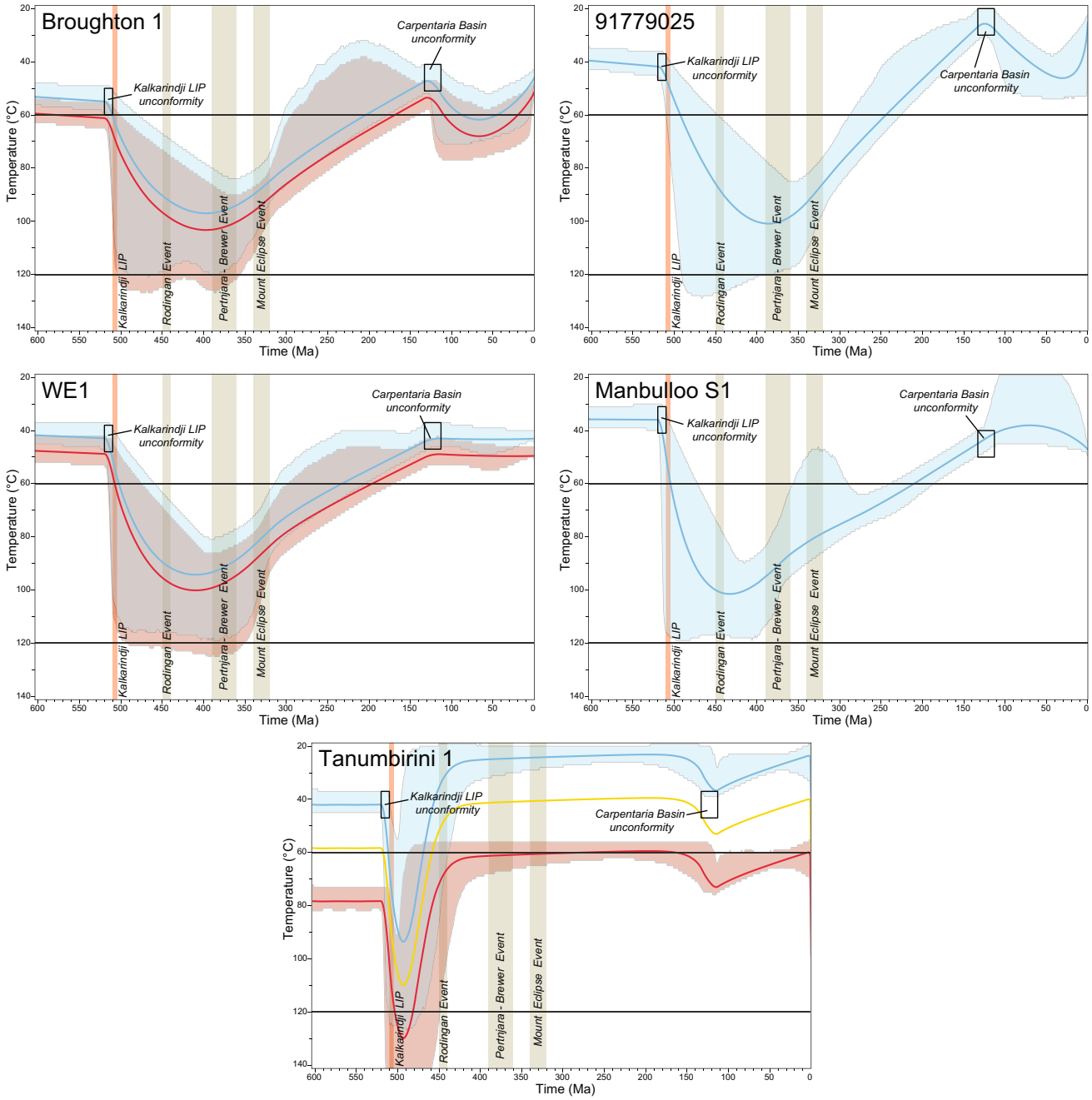

FIGURE 6 Low-temperature thermal history models for the McArthur Basin, produced using QTQt software (Gallagher, 2012). Solid lines denote the 'expected' thermal history, while associated envelops provide the 95% confidence interval. Blue paths represent the modelled thermal history of the shallowest sample, orange the intermediate and red the deepest (where applicable). Regional geology has been considered in modelling processes (Green & Duddy, 2021), where unconformities below the Kalkarindji LIP (Evins et al., 2009; Glass & Phillips, 2006; Jourdan et al., 2014; Macdonald et al., 2005) and Carpentaria Basin (Krassay, 1994) have been used to constrain sample temperature immediately prior to deposition of these units. The timing of magmatism of the Kalkarindji LIP (ca. 510 Ma) has been indicated, as well as the durations of deformational episodes of the Alice Springs Orogeny, including the Rodingan Event (ca. 450–440 Ma; Hand et al., 1999; Mawby et al., 1999; Shaw & Black, 1991), Pertnjara-Brewer Event (ca. 390–360 Ma; Ahmad & Munson, 2013; Bradshaw & Evans, 1988; Jones, 1972) and Mount Eclipse Event (ca. 340–320 Ma; Ahmad & Munson, 2013; Bradshaw & Evans, 1988). The apatite partial annealing zone between temperatures of 120–60°C (Gleadow et al., 1986; Wagner & Van den Haute, 1992) is indicated on each model.

well is consistent with models of peak hydrocarbon generation in the Beetaloo Sub-basin during the Cambrian (Faiz et al., 2021; RobSearch Australia, 1998; Taylor et al., 1994), when source rocks in the Velkerri Formation (Figure 2) in or near the oil window were elevated into the gas window. Basin heating driven by burial below high-temperature lavas and potential associated lithospheric thinning (Glass, 2002) provided a mechanism for raising

13652117, 2022, 6, Downloaded from https://onlinelibrary.wiley.com/doi/10.1111/bre.12691 by University of Adelaide Alumni, Wiley Online Library on [28/11/2022]. See the Terms and Conditions (https://onlinelibrary.wiley.com/terms-and-conditions) on Wiley Online Library for rules of use; OA articles are governed by the applicable Creative Commons License

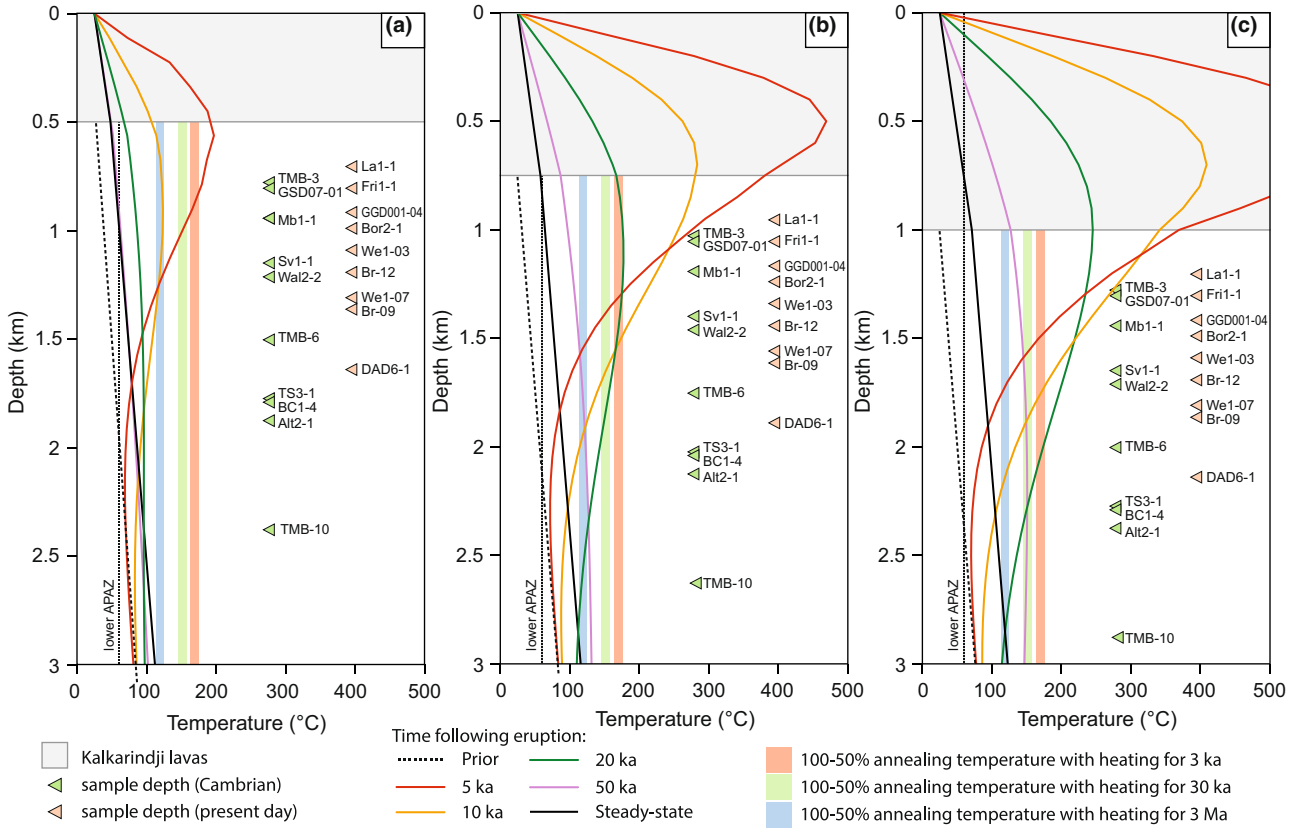

FIGURE 7 One-dimensional transient thermal modelling of McArthur Basin sediments in response to Kalkarindji LIP emplacement for lava thicknesses of (a) 500 m, (b) 750 m and (c) 1000 m. For each Kalkarindji thickness the one-dimensional thermal profile has been provided for time intervals following lava emplacement at time = 0 ka, such that the thermal profile for time = 5 ka represents crustal temperatures at 5 ka following initial lava extrusion, and so on. Additional geotherms for the thermal state prior to lava emplacement and steady-state geotherm expected with completely cooled lava overburden have further been shown. Temperature ranges required for 100%–50% annealing of tracks in apatite have been provided for multiple time durations, as calculated from fanning Arrhenius annealing model (Green et al., 1986; Laslett et al., 1987). Additionally, a lower temperature boundary for long-term partial annealing of fission tracks in apatite has provided at ca. 60°C (Gleadow et al., 1986; Wagner & Van den Haute, 1992). Vertical depth of drill hole samples have further been provided; for wells which preserve an unconformity between pre- and post-Kalkarindji strata samples have been normalised to reflect depth at time of Kalkarindji emplacement, while in wells which do not preserve Kalkarindji basalts or any post-Kalkarindji sediments the present day sample depth has been provided. It is possible, however, that these samples were deeper than present day-depth at time of the Kalkarindji eruption.

source rock temperatures into the oil and/or gas windows, and is further supported by observation of primary bitumen in sediment associated with Kalkarindji lavas in the Beetaloo Sub-basin (Matthews, 2008), although only source rocks very close to lava flows and reaching temperatures of ca. 200°C would have experienced significant hydrocarbon maturation across at the ka time-scale (Waples, 1980). Hence, we suggest that Kalkarindji extrusion, and more importantly subsequent Palaeozoic insulation heating, was likely to have instigated a second phase of hydrocarbon generation at least within and near the Beetaloo Sub-basin, following proposed initial generation in the Mesoproterozoic (Crick et al., 1988; Dutkiewicz et al., 2007; Taylor et al., 1994; Warren et al., 1998).

Thickened lava sequences observed in the eastern Beetaloo Sub-basin (Figure 8a) may be merely a consequence of greater local preservation, however, it is possible they are indeed reflective of differential Cambrian accumulation conditions. The shallowest depths to the erosional surface below the Kalkarindji lavas (normalised to remove Mesozoic–Cenozoic cover) in the northern Beetaloo region (Figure 8b) are coincident with thinner lava deposits (Figure 8a), while thickest lavas are correlated with deeper erosional horizons in the central Beetaloo Sub-basin (Hibbird, 1993a, 1993b; Menpes, 1993). If these correlations are representative of contemporary environments and flow thicknesses, it is plausible that the central Beetaloo Sub-basin was a subaerial topographic low during Kalkarindji LIP volcanism, while northern and eastern regions were elevated. This model would result in less magnitude of heating at the sub-basin margins from lava overburden, consistent with

13652117, 2022, 6, Downloaded from https://onlinelibrary.wiley.com/doi/10.1111/bre.12691 by University of Adelaide Alumni, Wiley Online Library on [28/11/2022]. See the Terms and Conditions (https://onlinelibrary.wiley.com/terms-and-conditions) on Wiley Online Library for rules of use; OA articles are governed by the applicable Creative Commons License

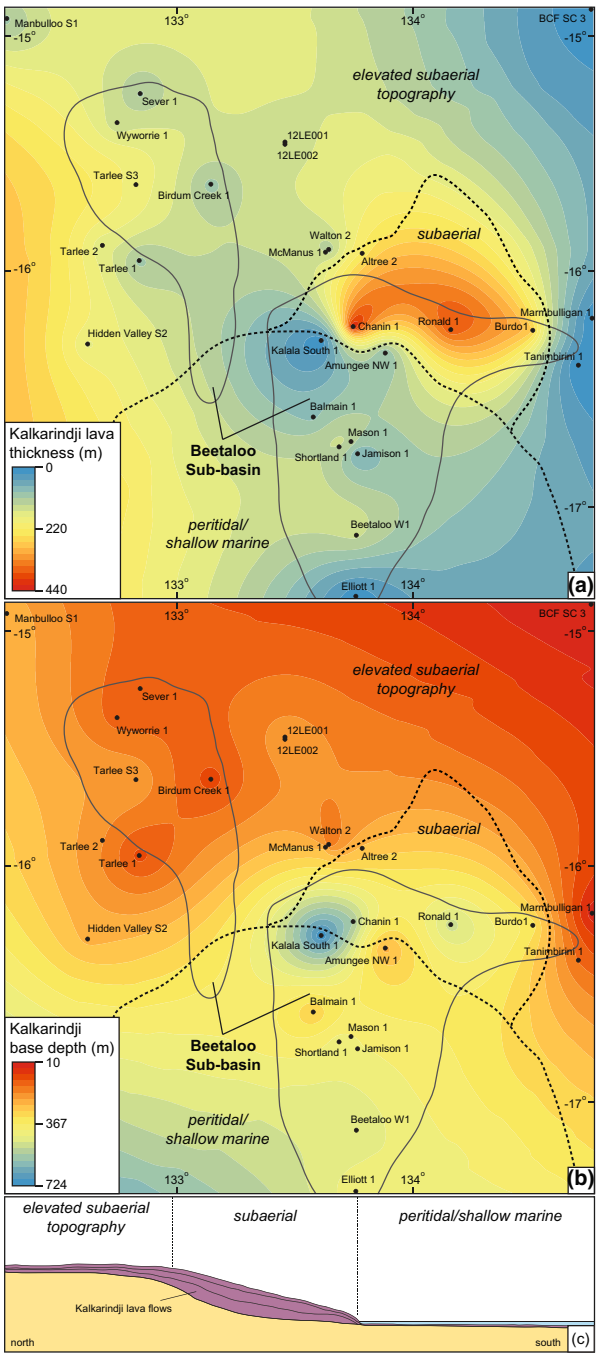

FIGURE 8 (a) Empirical Bayesian kriging interpolation for sub-surface thickness of Kalkarindji LIP lavas in the Beetaloo Sub-basin region, using thickness of lavas intersected by drill cores. (b) Empirical Bayesian kriging interpolation of sub-surface depth to the basal horizon of the Kalkarindji lava flows below Mesozoic–Cenozoic cover, as defined as the unconformable surface above the Kiana Group, or where absent, the unconformable surface above the McArthur Basin. Data for figures (a) and (b) were gathered from published drilling and log reports from the Beetaloo area (Adderly, 2015; Gaughan, 2013; Hibbird, 1993a, 1993b; Hibbird & Slater, 1992; Hokin, 2015; Lanigan, 1992; Lanigan & Ledlie, 1990a, 1990b; Lanigan & Torkington, 1991; Mackinlay, 2016; Menpes, 1992; Menpes, 1993; Origin Energy Resources, 2015a, 2015b, 2016; Pangaea Resources, 2014a, 2014b; Pangaea Resources, 2015a, 2015b; Pangaea Resources, 2016a, 2016b, 2016c; Torkington et al., 1989; Torkington & Derrington, 1992; Torkington & Lanigan, 1991). Cambrian regions of peritidal/shallow marine, subaerial and elevated subaerial topography have been inferred for the local environment during eruption of the Kalkarindji LIP. (c) Cartoon of Cambrian topography during eruption of Kalkarindji LIP, depicting relative lava flow thickness across the Beetaloo Sub-basin.

observation of gas generation in the central Beetaloo Sub-basin and lower temperature oil generation at sub-basin edges (RobSearch Australia, 1998). Furthermore, such a model suggests that the Tanumbirini 1 well was situated in slightly elevated topography on the eastern margin of the sub-basin, and therefore, basaltic flows may have been more easily eroded from this area (Figure 6). It remains unclear from hydrocarbon maturation data whether the Kalkarindji lavas similarly sparked renewed hydrocarbon generation beyond the Beetaloo Sub-basin (Dutkiewicz et al., 2007; Warren et al., 1998) however, our thermal history models for the central and northwestern McArthur Basin (Figures 5 and 6) suggests this as a distinct possibility.

The comparatively deep erosional horizon below the Kalkarindji LIP in the southern Beetaloo Sub-basin is not, however, matched by a thickening of sub-aerial lava flows as would be expected in a pure accommodation-space driven model (Figure 8a,b). This region of lower topography may therefore have been a peritidal to shallow marine environment opening towards the shallow marine depocentre of the southern Georgina Basin (Dunster et al., 2007; Kennard, 1991; Kruse & West, 1980), where oceanic waters largely prevented the continued flow of subaerial lavas as they would commonly crystallise rapidly to unconsolidated glass (Figure 8c; Moore et al., 1973). Kalkarindji lava emplacement in this region would have been controlled by local relative sea level, only advancing southwards during periods of marine regression.

5.2 | Palaeozoic denudation

Following eruption of the Kalkarindji LIP and heating to Cambrian peak temperatures, the Manbulloo S1, Broughton 1 and WE1 wells and field sample 91779025 experienced slow cooling between ca. 390–300 Ma (Figure 6). The timing of this cooling phase is broadly coincident with propagation of far-field stresses from the plate margins during the central Australian Alice Springs Orogeny (e.g., Buick et al., 2008; Haines et al., 2001; Hand et al., 1999; Raimondo et al., 2010; Shaw et al., 1992); specifically the later deformational episodes of the Pertnjara-Brewer Event (ca. 390–360 Ma; Ahmad & Munson, 2013; Bradshaw & Evans, 1988; Jones, 1972), and the Mount Eclipse Event (ca. 340–320 Ma; Ahmad & Munson, 2013;

13652117, 2022, 6, Downloaded from https://onlinelibrary.wiley.com/doi/10.1111/bre.12691 by University of Adelaide Alumni, Wiley Online Library on [28/11/2022]. See the Terms and Conditions (https://onlinelibrary.wiley.com/terms-and-conditions) on Wiley Online Library for rules of use; OA articles are governed by the applicable Creative Commons License

Bradshaw & Evans, 1988). The Manbulloo S1 well, near the Mallupunya Fault bordering the Pine Creek Orogen (Figures 1 and 6) records initiation of cooling contemporaneous with a ca. 400–350 Ma rapid cooling phase in the Pine Creek Orogen (Nixon, Glorie, Collins, Whelan, et al., 2021). Although the model records primarily slow cooling, we suggest that the initiation of cooling may be linked with reactivation of the Mallupunya Fault during the Pertnjara-Brewer Event (Ahmad & Munson, 2013; Bradshaw & Evans, 1988; Jones, 1972). The DAD0006 well and 91779016 field sample overlying shallow basement in the northwestern McArthur Basin (Figure 1) yield AFT central ages consistent with that of the Manbulloo S1 well (Figure 5), and likely also experienced accelerated denudation and cooling during the Pertnjara-Brewer Event with reactivation of structures associated with the Pine Creek Orogen basement.

Field sample 91779025 and the Broughton 1 and WE1 wells experienced cooling rates of ca. 0.3–0.2°C/Ma from ca. 390–300 Ma which are much slower than those typically observed in uplifted or incised terrains, but higher than for quiescent cratonic regimes (e.g., Fairbridge & Finkl, 1980; Summerfield & Hulton, 1994). Given these slow cooling rates, the samples from the central McArthur Basin appear to have not been significantly influenced by the Alice Springs Orogeny, and contrast with many thermal history profiles documented across northern Australia (e.g., Glorie, Agostino, et al., 2017; Nixon, Glorie, Collins, Whelan, et al., 2021; Spikings et al., 2006). Instead, we attribute Devonian–Carboniferous cooling in the central McArthur Basin to gradual erosion of overlying sediments and volcanics of the Georgina Basin and Kalkarindji LIP, which are now only sparsely preserved within the McArthur Basin region (Abbott et al., 2001; Ahmad & Munson, 2013; Dunn, 1963; Glass & Phillips, 2006). Unlike major structural reactivation observed in the adjacent Pine Creek Orogen and Murphy Province (Nixon, Glorie, Collins, Whelan, et al., 2021; Spikings et al., 2006), any Devonian–Carboniferous deformation in the McArthur Basin appears to have been minor, at most serving to elevate the region above the peritidal to shallow marine conditions experienced during Georgina Basin deposition (Kruse & Radke, 2008) and into subaerial exposure, without the creation of meaningful topographic relief.

5.3 | Mesozoic reheating

Thermal modelling for the Tanumbrini 1 and Broughton 1 wells predicts a minor Cretaceous reheating event (Figure 6) coincident with deposition in the overlying Carpentaria Basin (Abbott et al., 2001; Carson et al., 1999; McConachie et al., 1990). This heating event is relatively minor, and most likely induced by insulation from Carpentaria Basin sedimentary rocks, which subsequent cooling facilitated by gentle erosion of these strata once the region became emergent. Onshore sequences of the Carpentaria Basin are generally thin (Ahmad & Munson, 2013; McConachie et al., 1990), and coupled with thermal modelling results it thus appears unlikely that this sedimentation was responsible for any significant hydrocarbon maturation.

Our observations and interpretations of the Phanerozoic thermal history observed in this study are notably different to that proposed for the Broadmere 1 well in the eastern McArthur Basin (Duddy et al., 2004). Caution should be emphasised, however, in comparing thermal history models generated using different modelling approaches. The investigation by Duddy et al. (2004) proposed Jurassic cooling, Late Cretaceous reheating and subsequent Cenozoic cooling in Broadmere 1 that is not observed in our data from the wider region, and may instead be confined to the region approaching the Batten Fault Zone (Figure 1). Crick et al. (1988) note higher past heat flow and the presence of overmature hydrocarbons in the Batten Fault Zone, which similarly suggests the region experienced a contrasting thermal history to the wider basin. Mesozoic–Cenozoic denudation (Duddy et al., 2004) has stripped the majority of Phanerozoic sediments proximal to the fault zone, including potentially thickened Kalkarindji LIP sequences, which may have contributed to the observed elevated temperatures and advanced maturation of hydrocarbons (Crick et al., 1988). Understanding of the thermal evolution around the Batten Fault Zone, however, remains incomplete, but at present appears distinct from much of the rest of the McArthur Basin.

6 | CONCLUSIONS

New apatite fission track analysis has been conducted on 20 sample sites across the McArthur Basin, providing the most extensive thermal history study across the region yet conducted. Significant Cambrian heating associated with widespread emplacement of the Kalkarindji LIP at ca. 510 Ma is observed across the McArthur Basin, and may be responsible for a secondary phase of hydrocarbon generation within the region. Preserved Kalkarindji lavas are thickest in the central Beetaloo Sub-basin where they likely stimulated gas production in stratigaphically deeper source rocks as the sub-basin experienced elevated temperatures, although flows likely once covered much of the basin surface. Thermal disruption of the basin due to lava emplacement occurred

13652117, 2022, 6, Downloaded from https://onlinelibrary.wiley.com/doi/10.1111/bre.12691 by University of Adelaide Alumni, Wiley Online Library on [28/11/2022]. See the Terms and Conditions (https://onlinelibrary.wiley.com/terms-and-conditions) on Wiley Online Library for rules of use; OA articles are governed by the applicable Creative Commons License

across two distinct timescales, with initial shallow, high-magnitude heating of the sub-surface persisting for tens of thousands of years, while insulation of deeper basin sediments by basaltic flows equilibrated over millions of years. Subsequent deposition of Georgina Basin sediments above much of the McArthur Basin added to the thermal insulation of underlying strata, preserving elevated temperatures until widespread shallow erosion during the Devonian–Carboniferous. While initiation of cooling was coeval with the Alice Springs Orogeny, cooling was slow across most of the basin, and potential structural reactivation is only observed in the northeastern McArthur Basin, proximal to basement of the Pine Creek Orogen.

ACKNOWLEDGEMENTS

The authors acknowledge the Aboriginal Traditional Owners of the land on which this work was carried out. We further acknowledge Sarah Gilbert and Benjamin Wade for assistance with data collection. Morgan Blades assisted with sampling of core from wells GSD-7, GGD001, Broughton 1 and WE1, while samples 91779016 and 91779025 were provided by Geoscience Australia. This work has been supported by the Mineral Exploration Cooperative Research Centre (MinEx CRC) whose activities are funded by the Australian Government's Cooperative Research Centre Programme. This is MinEx CRC Document 2021/66. Research was additionally funded by an Australian Research Council Linkage Project (LP160101353), which is partnered by the Northern Territory Geological Survey, SANTOS Ltd, Origin Energy and Imperial Oil and Gas. The thermochronology laboratory where this research was conducted was funded via an Australian Research Council LIEF Project (LE150100145). Geoff Fraser publishes with the permission of the CEO, Geoscience Australia. Open access publishing facilitated by The University of Adelaide, as part of the Wiley - The University of Adelaide agreement via the Council of Australian University Librarians. Open access publishing facilitated by The University of Adelaide, as part of the Wiley - The University of Adelaide agreement via the Council of Australian University Librarians.

PEER REVIEW

The peer review history for this article is available at https://publons.com/publon/10.1111/bre.12691.

DATA AVAILABILITY STATEMENT

The data that support the findings of this study are available in the supplementary material of this article.

ORCID

Angus L. Nixon https://orcid.org/0000-0003-3638-1864

REFERENCES

Abbott, S. T., Sweet, I. P., Plumb, K. A., Young, D. N., Cutovinos, A., Ferenczi, P. A., Brakel, A. T., & Pietsch, B. A. (2001). *Roper Region: Urapunga—Roper River, Northern Territory: Combined explanatory notes, 1–107. (SD 53-10, 11)*. Northern Territory Geological Survey https://geoscience.nt.gov.au/gemis/ntgsjspui/handle/1/81859

Adderly, D. (2015). *Tanumbirini 1 interpreted well completion report. (PR2015-0034)*. Northern Territory Geological Survey https://geoscience.nt.gov.au/gemis/ntgsjspui/handle/1/83784

Ahmad, M., & Munson, T. J. (2013). *Geology and mineral resources of the Northern Territory*. Northern Territory Geological Survey, Special Publication 5.

Allison, K. R., & Sheehan, G. M. (1982). *EL 2888, Wearyan, annural report for 1982. (CR1982-0352)*. Northern Territory Geological Survey https://geoscience.nt.gov.au/gemis/ntgsjspui/handle/1/83784

Anderson, J. R., Lewis, C. J., Jarrett, A. J. M., Carr, L. K., Henson, P., Carson, C. J., Southby, C., & Munson, T. J. (2019). *New SHRIMP U–Pb zircon ages from the South Nicholson Basin, Mount Isa Province and Georgina Basin, Northern Territory and Queensland*, 1–101. (Record 2019/10). Geoscience Australia.

Barker, C. E. (1989). Temperature and time in the thermal maturation of sedimentary organic matter. In: N. D. Naeser & T. H. McCulloh (Eds.), *Thermal history of sedimentary basins* (pp. 73–98). Springer.

Bodorkos, S., Crowley, J. L., Claoué-Long, J. C., Anderson, J. R., & Magee, C. W. (2021). Precise U–Pb baddeleyite dating of the Derim Derim Dolerite, McArthur Basin, Northern Territory: Old and new SHRIMP and ID-TIMS constraints. *Australian Journal of Earth Sciences*, *68*, 36–50. https://doi.org/10.1080/08120099.2020.1749929

Boone, S. C., Seiler, C., Reid, A. J., Kohn, B., & Gleadow, A. (2016). An Upper Cretaceous paleo-aquifer system in the Eromanga Basin of the central Gawler Craton, South Australia: Evidence from apatite fission track thermochronology. *Australian Journal of Earth Sciences*, *63*, 315–331. https://doi.org/10.1080/08120099.2016.1199050

Bradshaw, J. D., & Evans, P. R. (1988). Palaeozoic tectonics, Amadeus Basin, central Australia. *The APPEA Journal*, *28*, 267–282. https://doi.org/10.1071/AJ87021

Buick, I. S., Storkey, A., & Williams, I. S. (2008). Timing relationships between pegmatite emplacement, metamorphism and deformation during the intra-plate Alice Springs Orogeny, central Australia. *Journal of Metamorphic Geology*, *26*, 915–936. https://doi.org/10.1111/j.1525-1314.2008.00794.x

Carson, C., Haines, P. W., Brakel, A. T., Pietsch, B. A., & Ferenczi, P. A. (1999). *Milingimbi, Northern Territory: Explanatory notes, 1–46. (SD 53-2)*. Northern Territory Geological Survey https://geoscience.nt.gov.au/gemis/ntgsjspui/handle/1/81863

Chapman, D. S. (1986). Thermal gradients in the continental crust. *Geological Society, London, Special Publications*, *24*, 63–70. https://doi.org/10.1144/gsl.Sp.1986.024.01.07

Chew, D. M., Babechuk, M. G., Cogné, N., Mark, C., O'Sullivan, G. J., Henrichs, I. A., Doepke, D., & McKenna, C. A. (2016). (LA,Q)-ICPMS trace-element analyses of Durango and McClure Mountain apatite and implications for making natural LA-ICPMS mineral standards. *Chemical Geology*, *435*, 35–48. https://doi.org/10.1016/j.chemgeo.2016.03.028

13652117, 2022, 6, Downloaded from https://onlinelibrary.wiley.com/doi/10.1111/bre.12691 by University of Adelaide Alumni, Wiley Online Library on [28/11/2022]. See the Terms and Conditions (https://onlinelibrary.wiley.com/terms-and-conditions) on Wiley Online Library for rules of use; OA articles are governed by the applicable Creative Commons License

Close, D. F. (2014). *The McArthur Basin: NTGS' aproach to a frontier petroleum basin with known base metal prospectivity, Annual Geoscience Exploration Seminar (AGES)* (pp. 85–89). Northern Territory Geological Survey.

Cox, G. M., Collins, A. S., Jarrett, A. J. M., Blades, M. L., Shannon, A. V., Yang, B., Farkas, J., Hall, P. A., O'Hara, B., Close, D., & Baruch, E. T. (2022). A very unconventional hydrocarbon play: The Mesoproterozoic Velkerri Formation of Northern Australia. *AAPG Bulletin*, *106*, 1213–1237. https://doi.org/10.1306/12162120148

Cox, G. M., Jarrett, A., Edwards, D., Crockford, P. W., Halverson, G. P., Collins, A. S., Poirier, A., & Li, Z. X. (2016). Basin redox and primary productivity within the Mesoproterozoic Roper Seaway. *Chemical Geology*, *440*, 101–114. https://doi.org/10.1016/j.chemgeo.2016.06.025

Crick, I. H., Boreham, C. J., Cook, A. C., & Powell, T. G. (1988). Petroleum geology and geochemistry of Middle Proterozoic McArthur Basin, Northern Australia II: Assessment of source rock potential. *AAPG Bulletin*, *72*, 1495–1514. https://doi.org/10.1306/703c99d8-1707-11d7-8645000102c1865d

Danielson, J. J., & Gesch, D. B. (2011). *Global multi-resolution terrain elevation data 2010 (GMTED2010). (2011-1073)*. U. S. Geological Survey http://pubs.er.usgs.gov/publication/ofr20111073

Donelick, R. A., & Miller, D. S. (1991). Enhanced TINT fission-track densities in low spontaneous track density apatites using 252Cf-derived fission fragment tracks: A model and experimenal observations. *Nuclear Tracks and Radiation Measurements*, *18*, 301–307.

Duddy, I. R., Green, P. F., Gibson, H. J., Hegarty, K. A., & Ellis, G. K. (2004). *Regional palaeo-thermal episodes in northern Australia, Timor Sea Petroleum Geoscience*. Proceedings of the Timor Sea Symposium, Darwin, Northern Territory, 19–20 June 2003, pp. 567–591.

Dunn, P. R. (1963). *Hodgson Downs, Northern Territory: Explanatory notes. (SD 53-14)*. Bureau of Mineral Resources, G.a.G. https://geoscience.nt.gov.au/gemis/ntgsjspui/handle/1/81764

Dunster, J. N., Kruse, P. D., Duffett, M. L., & Ambrose, G. J. (2007). *Geology and resource potential of the southern Georgina Basin, 1–232. (DIP007)*. Northern Territory Geological Survey https://geoscience.nt.gov.au/gemis/ntgsjspui/handle/1/81746

Dutkiewicz, A., Volk, H., Ridley, J., & George, S. C. (2007). Precambrian inclusion oils in the Roper Group: A review. In T. J. Munson & G. J. Ambrose (Eds.), *Central Australian Basins Symposium (CABS)* (pp. 326–348). Northern Territory Geological Survey.

Evins, L. Z., Jourdan, F., & Phillips, D. (2009). The Cambrian Kalkarindji Large Igneous Province: Extent and characteristics based on new 40Ar/39Ar and geochemical data. *Lithos*, *110*, 294–304. https://doi.org/10.1016/j.lithos.2009.01.014

Fairbridge, R. W., & Finkl, C. W. J. (1980). Cratonic erosional unconformities and peneplains. *The Journal of Geology*, *88*, 69–86. https://doi.org/10.1086/628474

Faiz, M., Crombez, V., Delle Piane, C., Lupton, N., Camilleri, M., & Langhi, L. (2021). *Petroleum systems model for source-rock-reservoir evauation in the Beetaloo Sub-basin*, 1–6. Conference Paper, 3rd AEGC: Geosciences for a Sustainable World, Brisbane, Australia.

Flowers, R. M., Farley, K. A., & Ketcham, R. A. (2015). A reporting protocol for thermochronologic modeling illustrated with data from the Grand Canyon. *Earth and Planetary Science Letters*, *432*, 425–435. https://doi.org/10.1016/j.epsl.2015.09.053

Frogtech Geoscience. (2018). *SEEBASE study and GIS for greater McArthur Basin. (DIP017)*. Northern Territory Geological Survey https://geoscience.nt.gov.au/gemis/ntgsjspui/handle/1/87064

Gallagher, K. (2012). Transdimensional inverse thermal history modeling for quantitative thermochronology. *Journal of Geophysical Research: Solid Earth*, *117*, 1–16. https://doi.org/10.1029/2011jb008825

Gard, M., Hasterok, D., & Halpin, J. A. (2019). Global whole-rock geochemical database compilation. *Earth System Science Data*, *11*, 1553–1566. https://doi.org/10.5194/essd-11-1553-2019

Gaughan, C. (2013). *Geophysics and drilling collaboration final report for EL27472 Larrimah East project 2012. (CR2012-1131)*. Northern Territory Geological Survey https://geoscience.nt.gov.au/gemis/ntgsjspui/handle/1/77200

George, S. C., & Ahmad, M. (2002). Use of aromatic compound distributions to evaluate organic maturity of the Proterozoic middle Velkerri Formation, McArthur Basin, Australia. In M. Keep & S. J. Moss (Eds.), *The Sedimentary Basins of Western Australia 3* (pp. 252–270). Proceedings of the Petroleum Exploration Society of Australia, Perth, Western Australia.

George, S. C., Llorca, S. M., & Hamilton, P. J. (1994). An integrated analytical approach for determining the origin of solid bitumens in the McArthur Basin, northern Australia. *Organic Geochemistry*, *21*, 235–248. https://doi.org/10.1016/0146-6380(94)90187-2

Glass, L. M. (2002). *Petrogenesis and geochronology of the North Australian Kalkarinji low-Ti continental flood basalt province*. (PhD thesis). Australian National University.

Glass, L. M., & Phillips, D. (2006). The Kalkarindji continental flood basalt province: A new Cambrian large igneous province in Australia with possible links to faunal extinctions. *Geology*, *34*, 461–464. https://doi.org/10.1130/g22122.1

Gleadow, A. J. W., Duddy, I. R., Green, P. F., & Lovering, J. F. (1986). Confined fission track lengths in apatite: A diagnostic tool for thermal history analysis. *Contributions to Mineralogy and Petrology*, *94*, 405–415. https://doi.org/10.1007/bf00376334

Glorie, S., Agostino, K., Dutch, R., Pawley, M., Hall, J., Danišík, M., Evans, N. J., & Collins, A. S. (2017). Thermal history and differential exhumation across the Eastern Musgrave Province, South Australia: Insights from low-temperature thermochronology. *Tectonophysics*, *703–704*, 23–41. https://doi.org/10.1016/j.tecto.2017.03.003

Glorie, S., Alexandrov, I., Nixon, A., Jepson, G., Gillespie, J., & Jahn, B. M. (2017). Thermal and exhumation history of Sakhalin Island (Russia) constrained by apatite U-Pb and fission track thermochronology. *Journal of Asian Earth Sciences*, *143*, 326–342. https://doi.org/10.1016/j.jseaes.2017.05.011

Glorie, S., Hall, J. W., Nixon, A., Collins, A. S., & Reid, A. (2019). Carboniferous fault reactivation at the northern margin of the metal-rich Gawler Craton (South Australia): Implications for ore deposit exhumation and preservation. *Ore Geology Reviews*, *115*, 103193. https://doi.org/10.1016/j.oregeorev.2019.103193

Green, P. F., & Duddy, I. R. (2021). Discussion: Extracting thermal history from low temperature thermochronology. A comment on recent exchanges between Vermeesch and Tian and Gallagher and Ketcham. *Earth-Science Reviews*, *216*, 103197. https://doi.org/10.1016/j.earscirev.2020.103197

13652117, 2022, 6, Downloaded from https://onlinelibrary.wiley.com/doi/10.1111/bre.12691 by University of Adelaide Alumni, Wiley Online Library on [28/11/2022]. See the Terms and Conditions (https://onlinelibrary.wiley.com/terms-and-conditions) on Wiley Online Library for rules of use; OA articles are governed by the applicable Creative Commons License

Green, P. F., Duddy, I. R., Gleadow, A. J. W., Tingate, P. R., & Laslett, G. M. (1986). Thermal annealing of fission tracks in apatite: 1. A qualitative description. *Chemical Geology*, *59*, 237–253. https://doi.org/10.1016/0168-9622(86)90074-6

Haines, P. W., Hand, M., & Sandiford, M. (2001). Palaeozoic synorogenic sedimentation in central and northern Australia: A review of distribution and timing with implications for the evolution of intracontinental orogens. *Australian Journal of Earth Sciences*, *48*, 911–928. https://doi.org/10.1046/j.1440-0952.2001.00909.x

Hall, J. W., Glorie, S., Collins, A. S., Reid, A., Evans, N., McInnes, B., & Foden, J. (2016). Exhumation history of the Peake and Denison Inliers: Insights from low-temperature thermochronology. *Australian Journal of Earth Sciences*, *63*, 805–820. https://doi.org/10.1080/08120099.2016.1253615

Hall, J. W., Glorie, S., Reid, A. J., Collins, A. S., Jourdan, F., Danišík, M., & Evans, N. (2018). Thermal history of the northern Olympic Domain, Gawler Craton; correlations between thermochronometric data and mineralising systems. *Gondwana Research*, *56*, 90–104. https://doi.org/10.1016/j.gr.2018.01.001

Hand, M., Mawby, J., Miller, J. A., Ballevre, M., Hensen, B. J., Moller, A., & Buick, I. S. (1999). Tectonothermal evolution of the Harts and Strangways Range Region, eastern Arunta Inlier, central Australia. *Geological Society of Australia, Specialist Group in Geochemistry, Mineralogy and Petrology, Field Guide*, *4*, 42.

Hasebe, N., Barbarand, J., Jarvis, K., Carter, A., & Hurford, A. J. (2004). Apatite fission-track chronometry using laser ablation ICP-MS. *Chemical Geology*, *207*, 135–145. https://doi.org/10.1016/j.chemgeo.2004.01.007

Hasebe, N., Tamura, A., & Arai, S. (2013). Zeta equivalent fission-track dating using LA-ICP-MS and examples with simultaneous U–Pb dating. *Island Arc*, *22*, 280–291. https://doi.org/10.1111/iar.12040

Hearing, T. W., Harvey, T. H. P., Williams, M., Leng, M. J., Lamb, A. L., Wilby, P. R., Gabbott, S. E., Pohl, A., & Donnadieu, Y. (2018). An early Cambrian greenhouse climate. *Science Advances*, *4*, eaar5690. https://doi.org/10.1126/sciadv.aar5690

Hibbird, S. A. (1993a). *Burdo 1 well completion report. (PR1993-0067)*. Northern Territory Geological Survey https://geoscience.nt.gov.au/gemis/ntgsjspui/handle/1/79292

Hibbird, S. A. (1993b). *Well completion report EP18—Chanin 1 Beetaloo Sub-Basin of the McArthur Basin. (PR1993-0043)*. Northern Territory Geological Survey https://geoscience.nt.gov.au/gemis/ntgsjspui/handle/1/79291

Hibbird, S. A., & Slater, J. (1992). *Well Completion Report EP18—Shortland 1 Beetaloo sub-basin of the McArthur Basin. (PR1992-0120)*. Northern Territory Geological Survey https://geoscience.nt.gov.au/gemis/ntgsjspui/handle/1/79438

Hokin, G. (2015). *Well completion report well BCFSC03 EP 184 McArthur Basin Northern Territory, Australia. (PR2014-0074)*. Northern Territory Geological Survey https://geoscience.nt.gov.au/gemis/ntgsjspui/handle/1/79840

Jackson, M. J., Powell, T. G., Summons, R. E., & Sweet, I. P. (1986). Hydrocarbon shows and petroleum source rocks in sediments as old as 1.7 ×10^9 years. *Nature*, *322*, 727. https://doi.org/10.1038/322727a0

Jackson, M. J., & Raiswell, R. (1991). Sedimentology and carbon-sulphur geochemistry of the Velkerri Formation, a mid-Proterozoic potential oil source in northern Australia. *Precambrian Research*, *54*, 81–108. https://doi.org/10.1016/0301-9268(91)90070-Q

Jackson, M. J., Sweet, I. P., & Powell, T. G. (1988). Studies on petroleum geology and geochemistry, Middle Proterozoic McArthur Basin, northern Australia I: Petroleum potential. *The APPEA Journal*, *28*, 283–302. https://doi.org/10.1071/AJ87022

Jochum, K. P., Weis, U., Stoll, B., Kuzmin, D., Yang, Q., Raczek, I., Jacob, D. E., Stracke, A., Birbaum, K., Frick, D. A., Günther, D., & Enzweiler, J. (2011). Determination of reference values for NIST SRM 610–617 glasses following ISO guidelines. *Geostandards and Geoanalytical Research*, *35*, 397–429. https://doi.org/10.1111/j.1751-908X.2011.00120.x

Jones, B. G. (1972). Upper Devonian to lower Carboniferous stratigraphy of the Pertnjara Group, Amadeus Basin, central Australia. *Journal of the Geological Society of Australia*, *19*, 229–249. https://doi.org/10.1080/14400957208527885

Jourdan, F., Hodges, K., Sell, B., Schaltegger, U., Wingate, M. T. D., Evins, L. Z., Söderlund, U., Haines, P. W., Phillips, D., & Blenkinsop, T. (2014). High-precision dating of the Kalkarindji large igneous province, Australia, and synchrony with the Early–Middle Cambrian (Stage 4–5) extinction. *Geology*, *42*, 543–546. https://doi.org/10.1130/g35434.1

Kennard, J. M. (1991). *Lower Cambrian archaeocyathan build-ups, Todd River Dolomite, northeast Amadeus Basin, central Australia: Sedimentology and diagenesis, 195–225. (Bulletin 236)*. Bureau of Mineral Resources https://ui.adsabs.harvard.edu/abs/1991ggsa.rept.195K

Kositcin, N., Munson, T. J., & Whelan, J. A. (2017). *Summary of results*. Joint NTGS-GA geochronology project: Greater McArthur Basin, July 2016–June 2017. (NTGS Record 2017-012). Record. https://geoscience.nt.gov.au/gemis/ntgsjspui/handle/1/86834

Krassay, A. A. (1994). *The Cretaceous geology of northeastern Arnhem Land, Northern Territory. (Record 1994/40)*. Australian Geological Survey Organisation.

Kruse, P. D., & Radke, B. M. (2008). *Ranken—Avon Downs, Northern Territory: Explanatory notes, 1-41. (SE 53-16, SF 53-04)*. Northern Territory Geological Survey https://geoscience.nt.gov.au/gemis/ntgsjspui/handle/1/81892

Kruse, P. D., & West, P. W. (1980). Archaeocyatha of the Amadeus and Georgina Basins. *BMR Journal of Australian Geology & Geophysics*, *5*, 165–181.

Kruse, P. D., Wygralak, A. S., Sweet, P. D., Stuart-Smith, P. G., Pieters, P. E., & Crick, I. H. (1994). *Katherine, Northern Territory: Explanatory notes, 1–69. (SD 53-9)*. Northern Territory Geological Survey https://geoscience.nt.gov.au/gemis/ntgsjspui/handle/1/81894

Lanigan, K. (1992). *Well completion report EP33—Elliott 1 Beetaloo sub-basin of the McArthur Basin. (PR1992-0012)*. Northern Territory Geological Survey https://geoscience.nt.gov.au/gemis/ntgsjspui/handle/1/79452

Lanigan, K., Hibbird, S., Menpes, S., & Torkington, J. (1994). Petroleum exploration in the Proterozoic Beetaloo Sub-baisn, Northern Territory. *The APPEA Journal*, *34*, 674–691. https://doi.org/10.1071/AJ93050

Lanigan, K., & Ledlie, I. M. (1990a). *McManus 1 EP24 McArthur Basin, Northern Territory well completion report. (PR1989-0086)*. Northern Territory Geological Survey https://geoscience.nt.gov.au/gemis/ntgsjspui/handle/1/79425

Lanigan, K., & Ledlie, I. M. (1990b). *Walton 1-2 EP24 McArthur Basin, Northern Territory well completion report. (PR1989-0088)*.

13652117, 2022, 6, Downloaded from https://onlinelibrary.wiley.com/doi/10.1111/bre.12691 by University of Adelaide Alumni, Wiley Online Library on [28/11/2022]. See the Terms and Conditions (https://onlinelibrary.wiley.com/terms-and-conditions) on Wiley Online Library for rules of use; OA articles are governed by the applicable Creative Commons License

Northern Territory Geological Survey https://geoscience.nt.gov.au/gemis/ntgsjspui/handle/1/79496

Lanigan, K., & Torkington, J. (1991). *Well completion report EP19—Sever 1 Daly sub-basin of the McArthur Basin. (PR1990-0069)*. Northern Territory Geological Survey https://geoscience.nt.gov.au/gemis/ntgsjspui/handle/1/79258

Laslett, G. M., Green, P. F., Duddy, I. R., & Gleadow, A. J. W. (1987). Thermal annealing of fission tracks in apatite 2. A quantitative analysis. *Chemical Geology*, *65*, 1–13. https://doi.org/10.1016/0168-9622(87)90057-1

Macdonald, F. A., Wingate, M. T. D., & Mitchell, K. (2005). Geology and age of the Glikson impact structure, Western Australia. *Australian Journal of Earth Sciences*, *52*, 641–651. https://doi.org/10.1080/08120090500170419

Mackinlay, M. (2016). *Marmbulligan 1 basic well completion report. (PR2017-W002)*. Northern Territory Geological Survey https://geoscience.nt.gov.au/gemis/ntgsjspui/handle/1/87789

Markov, J., Foss, C., Swierczek, E., & Delle Piane, C. (2021). *Kalkarindji through the geophysical lens: Structural characteristics of the Kalkarindji basalt from non-seismic geophysical data*, 43–47. Annual Geoscience Exploration Seminar (AGES) 2021, Alice Springs, Australia.

Marks, M. A. W., Wenzel, T., Whitehouse, M. J., Loose, M., Zack, T., Barth, M., Worgard, L., Krasz, V., Eby, G. N., Stosnach, H., & Markl, G. (2012). The volatile inventory (F, Cl, Br, S, C) of magmatic apatite: An integrated analytical approach. *Chemical Geology*, *291*, 241–255. https://doi.org/10.1016/j.chemgeo.2011.10.026

Matthews, I. (2008). *Sturt Plateau Bitumen (SPB) project. Annual report EL's for the period 1 September 2007 to 1 September 2008. (CR2008-0375)*. Northern Territory Geological Survey https://geoscience.nt.gov.au/gemis/ntgsjspui/handle/1/74552

Mawby, J., Hand, M., & Foden, J. (1999). Sm-Nd evidence for high grade Ordovician metamorphism in the Arunta Block, Central Australia. *Journal of Metamorphic Geology*, *17*, 653–668. https://doi.org/10.1046/j.1525-1314.1999.00224.x

McConachie, B. A., Filatoff, J., & Senapati, N. (1990). Stratigraphy and petroleum potential of the onshore Carpentaria Basin, Queensland. *The APPEA Journal*, *30*, 149–164. https://doi.org/10.1071/AJ89009

McDannell, K. T. (2020). Notes on statistical age dispersion in fission-track datasets: The chi-square test, annealing variability, and analytical considerations. *EarthArXiv*.

McDowell, F. W., McIntosh, W. C., & Farley, K. A. (2005). A precise Ar-40-Ar-39 reference age for the Durango apatite (U-Th)/He and fission-track dating standard. *Chemical Geology*, *214*, 249–263. https://doi.org/10.1016/j.chemgeo.2004.10.002

Menpes, S. A. (1992). *Well completion report EP18—Balmain 1. (PR1992-0122)*. Northern Territory Geological Survey https://geoscience.nt.gov.au/gemis/ntgsjspui/handle/1/79434

Menpes, S. A. (1993). *Well completion report EP18—Ronald 1. (PR1993-0056)*. Northern Territory Geological Survey https://geoscience.nt.gov.au/gemis/ntgsjspui/handle/1/79423

Merdith, A. S., Williams, S. E., Collins, A. S., Tetley, M. G., Mulder, J. A., Blades, M. L., Young, A., Armistead, S. E., Cannon, J., Zahirovic, S., & Müller, R. D. (2021). Extending full-plate tectonic models into deep time: Linking the Neoproterozoic and the Phanerozoic. *Earth-Science Reviews*, *214*, 103477. https://doi.org/10.1016/j.earscirev.2020.103477

Moore, J. G., Phillips, R. L., Grigg, R. W., Peterson, D. W., & Swanson, D. A. (1973). Flow of lava into the Sea, 1969–1971, Kilauea Volcano, Hawaii. *GSA Bulletin*, *84*, 537–546. https://doi.org/10.1130/0016-7606(1973)84<537:Folits>2.0.Co;2

Mory, A. J., & Beere, G. M. (1988). *Geology of the onshore Bonaparte and Ord Basins in Western Australia. (Bulletin 134)*. Geological Survey of Western Australia.

Munson, T. J. (2016). *Sedimentary characterisation of the Wilton package, greater McArthur Basin, Northern Territory, 1–151. (NTGS Record 2016-003)*. Northern Territory Geological Survey https://geoscience.nt.gov.au/gemis/ntgsjspui/handle/1/82741

Nixon, A. L., Glorie, S., Collins, A. S., Blades, M. L., Simpson, A., & Whelan, J. A. (2021). Inter-cratonic geochronological and geochemical correlations of the Derim Derim–Galiwinku/Yanliao reconstructed Large Igneous Province across the North Australian and North China cratons. *Gondwana Research*, *103*, 473–486. https://doi.org/10.1016/j.gr.2021.10.027

Nixon, A. L., Glorie, S., Collins, A. S., Whelan, J. A., Reno, B. L., Danišík, M., Wade, B. P., & Fraser, G. (2021). Footprints of the Alice Springs Orogeny preserved in far northern Australia: An application of multi-kinetic thermochronology in the Pine Creek Orogen and Arnhem Province. *Journal of the Geological Society*, *178*, jgs2020-2173. https://doi.org/10.1144/jgs2020-173

O'Sullivan, P. B., & Parrish, R. R. (1995). The importance of apatite composition and single-grain ages when interpreting fission track data from plutonic rocks: A case study from the Coast Ranges, British Columbia. *Earth and Planetary Science Letters*, *132*, 213–224. https://doi.org/10.1016/0012-821X(95)00058-K

Origin Energy Resources. (2015a). *Amungee NW-1H well completion report (basic), EP 98 Beetaloo Basin, Northern Territory. (PR2016-W001)*. Northern Territory Geological Survey https://geoscience.nt.gov.au/gemis/ntgsjspui/handle/1/87095

Origin Energy Resources. (2015b). *Kalala S-1 well completion report (basic), EP 98 Beetaloo Basin, Northern Territory. (PR2016-W013)*. Northern Territory Geological Survey https://geoscience.nt.gov.au/gemis/ntgsjspui/handle/1/86448

Origin Energy Resources. (2016). *Beetaloo W-1 well completion report (basic), EP 117 Beetaloo Basin, Northern Territory. (PR2017-W004)*. Northern Territory Geological Survey https://geoscience.nt.gov.au/gemis/ntgsjspui/handle/1/87095

Pangaea Resources. (2014a). *Basic well completion report NT EP167 Tarlee S3. (PR2015-0016)*. Northern Territory Geological Survey https://geoscience.nt.gov.au/gemis/ntgsjspui/handle/1/83524

Pangaea Resources. (2014b). *Basic well completion report, NT EP168, Hidden Valley S2. (PR2015-0015)*. Northern Territory Geological Survey https://geoscience.nt.gov.au/gemis/ntgsjspui/handle/1/83245

Pangaea Resources. (2015a). *Basic well completion report NT EP167 Birdum Creek 1. (PR2016-W006)*. Northern Territory Geological Survey https://geoscience.nt.gov.au/gemis/ntgsjspui/handle/1/86120

Pangaea Resources. (2015b). *Basic well completion report, NT EP167, Manbulloo S1. (PR2015-0017)*. Northern Territory Geological Survey https://geoscience.nt.gov.au/gemis/ntgsjspui/handle/1/83784

Pangaea Resources. (2016a). *Basic well completion report NT EP168 Tarlee 1. (PR2016-W002)*. Northern Territory Geological Survey https://geoscience.nt.gov.au/gemis/ntgsjspui/handle/1/86116

13652117, 2022, 6, Downloaded from https://onlinelibrary.wiley.com/doi/10.1111/bre.12691 by University of Adelaide Alumni, Wiley Online Library on [28/11/2022]. See the Terms and Conditions (https://onlinelibrary.wiley.com/terms-and-conditions) on Wiley Online Library for rules of use; OA articles are governed by the applicable Creative Commons License

Pangaea Resources. (2016b). *Basic well completion report NT EP168 Tarlee 2. (PR2016-W001)*. Northern Territory Geological Survey https://geoscience.nt.gov.au/gemis/ntgsjspui/handle/1/86259

Pangaea Resources. (2016c). *Basic well completion report, NT EP167, Wyworrie 1. (PR2016-W007)*. Northern Territory Geological Survey https://geoscience.nt.gov.au/gemis/ntgsjspui/handle/1/86440

Paton, C., Hellstrom, J., Paul, B., Woodhead, J., & Hergt, J. (2011). Iolite: Freeware for the visualisation and processing of mass spectrometric data. *Journal of Analytical Atomic Spectrometry*, *26*, 2508–2518. https://doi.org/10.1039/C1JA10172B

Quentin de Gromard, R., Kirkland, C. L., Howard, H. M., Wingate, M. T. D., Jourdan, F., McInnes, B. I. A., Danišík, M., Evans, N. J., McDonald, B. J., & Smithies, R. H. (2019). When will it end? Long-lived intracontinental reactivation in central Australia. *Geoscience Frontiers*, *10*, 149–164. https://doi.org/10.1016/j.gsf.2018.09.003

Raimondo, T., Collins, A. S., Hand, M., Walker-Hallam, A., Smithies, R. H., Evins, P. M., & Howard, H. M. (2010). The anatomy of a deep intracontinental orogen. *Tectonics*, *29*, TC4024. https://doi.org/10.1029/2009tc002504

Rawlings, D. J. (1999). Stratigraphic resolution of a multiphase intracratonic basin system: The McArthur Basin, northern Australia. *Australian Journal of Earth Sciences*, *46*, 703–723. https://doi.org/10.1046/j.1440-0952.1999.00739.x

Reddy, M., Glorie, S., Reid, A., & Collins, A. S. (2015). Phanerozoic cooling history of the central Gawler Craton: Implications of new low-temperature thermochronological data. *MESA Journal*, *75*, 56–60.

RobSearch Australia. (1998). *Technical review of EP18 and EP(A)70 Beetaloo Basin, Northern Territory. (PR1989-0034)*. Northern Territory Geological Survey https://geoscience.nt.gov.au/gemis/ntgsjspui/handle/1/89027

Shaw, R. D., & Black, L. P. (1991). The history and tectonic implications of the Redbank Thrust Zone, central Australia, based on structural, metamorphic and Rb-Sr isotopic evidence. *Australian Journal of Earth Sciences*, *38*, 307–332. https://doi.org/10.1080/08120099108727975

Shaw, R. D., Zeitler, P. K., McDougall, I., & Tingate, P. R. (1992). The Palaeozoic history of an unusual intracratonic thrust belt in central Australia based on 40Ar-39Ar, K-Ar and fission track dating. *Journal of the Geological Society*, *149*, 937–954. https://doi.org/10.1144/gsjgs.149.6.0937

Smith, T., Kelman, A. P., Nicoll, R., Edwards, D., Hall, L., Laurie, J., & Carr, L. (2013). An updated stratigraphic framework for the Georgina Basin, NT and Queensland. *The APPEA Journal*, *53*, 487. https://doi.org/10.1071/AJ12098

Spikings, R. A., Foster, D. A., & Kohn, B. P. (2006). Low-temperature (<110°C) thermal history of the Mt Isa and Murphy Inliers, northeast Australia: Evidence from apatite fission track thermochronology. *Australian Journal of Earth Sciences*, *53*, 151–165. https://doi.org/10.1080/08120090500434609

Summerfield, M. A., & Hulton, N. J. (1994). Natural controls of fluvial denudation rates in major world drainage basins. *Journal of Geophysical Research: Solid Earth*, *99*, 13871–13883. https://doi.org/10.1029/94JB00715

Summons, R. E., Powell, T. G., & Boreham, C. J. (1988). Petroleum geology and geochemistry of the Middle Proterozoic McArthur Basin, Northern Australia: III. Composition of extractable hydrocarbons. *Geochimica Et Cosmochimica Acta*, *52*, 1747–1763. https://doi.org/10.1016/0016-7037(88)90001-4

Sweet, I. P., Brakel, A. T., Rawlings, D. J., Haines, P. W., Plumb, K. A., & Wygralak, A. S. (1999). *Mount Marumba, Northern Territory: Explanatory notes, 1–84. (SD 53-6)*. Northern Territory Geological Survey https://geoscience.nt.gov.au/gemis/ntgsjspui/handle/1/81911

Taylor, D., Kontorovich, A. E., Larichev, A. I., & Glikson, M. (1994). Petroleum source rocks in the Roper Group of the McArthur Basin: Source characterisation and maturity determinations using physical and chemical methods. *The APPEA Journal*, *34*, 279–296. https://doi.org/10.1071/AJ93026

Tingate, P. R., & Duddy, I. R. (2002). The thermal history of the eastern Officer Basin (South Australia): Evidence from apatite fission track analysis and organic maturity data. *Tectonophysics*, *349*, 251–275. https://doi.org/10.1016/S0040-1951(02)00056-2

Tissot, B., Durand, B., Espitalié, J., & Combaz, A. (1974). Influence of nature and diagenesis of organic matter in formation of petroleum. *AAPG Bulletin*, *58*, 499–506. https://doi.org/10.1306/83d91425-16c7-11d7-8645000102c1865d

Torkington, J., & Derrington, S. (1992). *Well completion report EP18—Mason 1 Beetaloo sub-basin of the McArthur Basin. (PR1992-0027)*. Northern Territory Geological Survey https://geoscience.nt.gov.au/gemis/ntgsjspui/handle/1/79430

Torkington, J., & Lanigan, K. (1991). *Well completion report EP18—Jamison 1 Beetaloo sub-basin of the McArthur Basin. (PR1991-0020)*. Northern Territory Geological Survey https://geoscience.nt.gov.au/gemis/ntgsjspui/handle/1/79447

Torkington, J., & Ledlie, I. M. (1988). *Broughton 1 EP 5 McArthur Basin, Northern Territory well completion report. (PR1988-0078)*. Northern Territory Geological Survey https://geoscience.nt.gov.au/gemis/ntgsjspui/handle/1/83784

Torkington, J., Weste, G., Chiuoka, J., & Ledlie, I. M. (1989). *Altree-1 and 2 EP 24 McArthur Basin, Northern Territory well completion report. (PR1989-0016)*. Northern Territory Geological Survey https://geoscience.nt.gov.au/gemis/ntgsjspui/handle/1/79421

Vermeesch, P. (2017). Statistics for LA-ICP-MS based fission track dating. *Chemical Geology*, *456*, 19–27. https://doi.org/10.1016/j.chemgeo.2017.03.002

Vermeesch, P. (2018). IsoplotR: A free and open toolbox for geochronology. *Geoscience Frontiers*, *9*, 1479–1493. https://doi.org/10.1016/j.gsf.2018.04.001

Wagner, G. A., & Van den Haute, P. (1992). *Fission-track dating*. Kluwer Academic.

Walter, M. R., Veevers, J. J., Calver, C. R., & Grey, K. (1995). Neoproterozoic stratigraphy of the Centralian Superbasin, Australia. *Precambrian Research*, *73*, 173–195. https://doi.org/10.1016/0301-9268(94)00077-5

Waples, D. W. (1980). Time and temperature in petroleum formation: Application of Lopatin's method to petroleum exploration. *AAPG Bulletin*, *64*, 916–926. https://doi.org/10.1306/2f9193d2-16ce-11d7-8645000102c1865d

Warren, J. K., George, S. C., Hamilton, P. J., & Tingate, P. (1998). Proterozoic source rocks: Sedimentology and organic characteristics of the Velkerri Formation, Northern Territory, Australia1. *AAPG Bulletin*, *82*, 442–463. https://doi.org/10.1306/1d9bc435-172d-11d7-8645000102c1865d

Wells, A. T. (1970). *Geology of the Amadeus basin, central Australia*. Bureau of Mineral Resources, Geology and Geophysics, Bulletin 100.

13652117, 2022, 6, Downloaded from https://onlinelibrary.wiley.com/doi/10.1111/bre.12691 by University of Adelaide Alumni, Wiley Online Library on [28/11/2022]. See the Terms and Conditions (https://onlinelibrary.wiley.com/terms-and-conditions) on Wiley Online Library for rules of use; OA articles are governed by the applicable Creative Commons License

Wotte, T., Skovsted, C. B., Whitehouse, M. J., & Kouchinsky, A. (2019). Isotopic evidence for temperate oceans during the Cambrian Explosion. *Scientific Reports*, *9*, 6330. https://doi.org/10.1038/s41598-019-42719-4

Yang, B., Collins, A. S., Blades, M. L., Munson, T. J., Payne, J. L., Glorie, S., & Farkaš, J. (2020). Tectonic controls on sedimentary provenance and basin geography of the Mesoproterozoic Wilton package, McArthur Basin, northern Australia. *Geological Magazine*, *159*, 1–20. https://doi.org/10.1017/S0016756820001223

Yang, B., Collins, A. S., Cox, G. M., Jarrett, A. J. M., Denyszyn, S. W., Blades, M. L., Farkaš, J., & Glorie, S. (2020). Using Mesoproterozoic sedimentary geochemistry to reconstruct basin tectonic geography and link organic carbon productivity to nutrient flux from a Northern Australian large igneous Province. *Basin Research*, *32*, 1734–1750. https://doi.org/10.1111/bre.12450

Yang, B., Smith, T. M., Collins, A. S., Munson, T. J., Schoemaker, B., Nicholls, D., Cox, G., Farkas, J., & Glorie, S. (2018). Spatial and temporal variation in detrital zircon age provenance of the hydrocarbon-bearing upper Roper Group, Beetaloo Sub-basin, Northern Territory, Australia. *Precambrian Research*, *304*, 140–155. https://doi.org/10.10164/j.precamres.2017.10.025

SUPPORTING INFORMATION

Additional supporting information can be found online in the Supporting Information section at the end of this article.

How to cite this article: Nixon, A. L., Glorie, S., Hasterok, D., Collins, A. S., Fernie, N., & Fraser, G. (2022). Low-temperature thermal history of the McArthur Basin: Influence of the Cambrian Kalkarindji Large Igneous Province on hydrocarbon maturation. *Basin Research*, *34*, 1936–1959. https://doi.org/10.1111/bre.12691

13652117, 2022, 6, Downloaded from https://onlinelibrary.wiley.com/doi/10.1111/bre.12691 by University of Adelaide Alumni, Wiley Online Library on [28/11/2022]. See the Terms and Conditions (https://onlinelibrary.wiley.com/terms-and-conditions) on Wiley Online Library for rules of use; OA articles are governed by the applicable Creative Commons License